University of Stuttgart
Germany

Faculty 6: Aerospace Engineering and Geodesy

Annual Report **2020**

Geodesy & Geoinformatics

IIGS GIS INS ifp

editing and layout:
volker walter, markus antoni, martin metzner, aloysius wehr

Dear friends and colleagues,

It is our great pleasure to present to you this annual report on the 2020 activities and academic highlights of the Department of Geodesy and Geoinformatics of the University of Stuttgart. The Department consists of the four institutes:

- Institute of Geodesy (GIS),
- Institute for Photogrammetry (ifp),
- Institute of Navigation (INS),
- Institute of Engineering Geodesy (IIGS),

and is part of the Faculty of Aerospace Engineering and Geodesy.

Preface

This year was dominated by the Corona pandemic, which of course also influenced our research and teaching. Teaching in the summer and winter semesters was only possible online and research was also partly restricted due to the difficult boundary conditions. Nevertheless, we were able to offer all courses and the research projects were also successfully continued within the scope of the possibilities.

Research

This annual report documents our research contributions in many diverse fields of Geodesy and Geoinformatics: from satellite and physical geodesy through navigation, remote sensing, engineering surveying and telematics to photogrammetry, geographical information systems and location based services. Detailed information on projects and research output can be found in the following individual institutes' sections.

Teaching

We were able to welcome 21 new BSc students in winter term 2019/2020 (initially 34 students enrolled). For the first semester of the MSc program for Geodesy and Geoinformatics 7 students enrolled and we welcomed 7. Please visit our website www.geodaesie.uni-stuttgart.de for additional information on the programs.

Our successful international MSc program Geomatics Engineering (GeoEngine) exists already 15 years. Probably due establishment of tuition fees for non-EU students in 2018, we saw a decline of new students since then. Like last year, 37 people enrolled for the study programme this year. However, we welcomed only six students compared to 19 in 2019. We believe one reason for the decline in the number of students actually showing up could be a general reluctance to study abroad in times of pandemic.

Awards and Scholarships

We want to express our gratitude to our friends and sponsors, most notably:

- Verein Freunde des Studienganges Geodäsie und Geoinformatik an der Universität Stuttgart e.V. (F2GeoS),
- Ingenieur-Gesellschaft für Interfaces mbH (IGI),
- DVW Landesverein Baden-Württemberg,

who support our programs and our students with scholarships, awards and travel support. Below is the list of the recipients of the 2020 awards and scholarships. The criterion for all prizes is academic performance; for some prizes GPA-based, for other prizes based on thesis work. Congratulations to all recipients!

Uwe Sörgel, Associate Dean (Academic)

Uwe.soergel@ifp.uni-stuttgart.de

Award	**Recipient**	**Sponsor**	**Programme**
Karl-Ramsayer Preis	not awarded in 2020	Department of Geodesy & Geoinformatics	Geodesy & Geoinformatics
BSc Thesis Award	Ms Yifei Yin	F2GeoS	Geodesy & Geoinformatics
MSC Thesis Award	Mr. Roman Buss	F2GeoS	Geodesy & Geoinformatics

Institute of Engineering Geodesy

Geschwister-Scholl-Str. 24 D
70174 Stuttgart
Germany
Tel.: +49 711 685 84041
Fax: +49 711 685 84044
sekretariat@iigs.uni-stuttgart.de or
firstname.secondname@iigs.uni-stuttgart.de
http://https://www.iigs.uni-stuttgart.de/

Head of Institute

Prof. Dr.-Ing. habil. Dr. h.c. Volker Schwieger

Secretary

Elke Rawe
Désirée Schreib

Scientific Staff

M.Sc. Laura Balangé	Quality Modeling
M.Sc. Urs Basalla	Terrestrial Laser Scanning
M.Sc. Aiham Hassan (until 30.06.2020)	Monitoring
Dipl.-Ing. Susanne Haußmann (since 01.11.2020)	Kinematic Positioning
M.Sc. Gabriel Kerekes	Terrestrial Laser Scanning
Dr.-Ing. Otto Lerke	Machine Guidance
M.Sc. Philipp Luz	Digital Map
Dr.-Ing. Martin Metzner	Engineering Geodesy
M.Sc. Martin Wachsmuth (until 31.10.2020)	Kinematic Positioning
M.Sc. Jinyue Wang (until 31.03.2020)	Map Matching
Dr.-Ing. Li Zhang	Monitoring
Dr.-Ing. Yin Zhang	Engineering Geodesy

Technical Staff

Dipl.-Ing. (FH) Andreas Kanzler
Martin Knihs, Mechanikermeister
Dipl.-Geogr. Lars Plate

External Teaching Staff

Dipl.-Ing. Jürgen Eisenmann	Geschäftsbereichsleiter Landratsamt Ostalbkreis, Geoinformation und Landentwicklung
Dipl.-Ing. Christian Helfert	Fachdienstleiter Flurneuordnung im Landkreis Biberach
Dipl.-Math. Ulrich Völter	Geschäftsführer der Fa. Intermetric
Dr.-Ing. Thomas Wiltschko	Daimler AG, Mercedes-Benz Cars; Research and Development

PhD-Students

M.Sc. Julia Aichinger	Terrestrial Laser Scanning
M.Sc. Alexandra Avram	GNSS
M.Sc. Marko Gasparac	GNSS and Digital Map
Dipl.-Ing. Patric Hindenberger	Location Referencing
M.Sc. Yu Li	Digital Map
M.Sc. Dung Trung Pham (until 28.05.2020)	Kinematic Positioning
M.Sc. Annette Schmitt	Multi-Sensor-Systems
M.Sc. Tobias Schröder	Automation of Production Process
M.Sc. Yihui Yang	Multi-Sensor-Systems
M.Sc. Christian Bader	Kinematic Laser Scanning

General View

The Institute of Engineering Geodesy (IIGS) is directed by Prof. Dr.-Ing. habil. Dr. h.c. Volker Schwieger. It is part of Faculty 6 "Aerospace Engineering and Geodesy" within the University of Stuttgart. Prof. Schwieger holds the chair in "Engineering Geodesy and Geodetic Measurements". Since 2017, he is the Dean of Faculty 6.

In addition to being a member of Faculty 6, Prof. Schwieger is co-opted to Faculty 2 "Civil and Environmental Engineering". Furthermore, the IIGS is involved in the Center for Transportation Research of the University of Stuttgart (FOVUS). Thus, the IIGS actively continues the close collaboration with all institutes in the field of transportation, especially with those belonging to Faculty 2.

Since 2011, Prof. Schwieger is a full member of the German Geodetic Commission (Deutsche Geodätische Kommission - DGK). Furthermore, he is head of the section "Engineering Geodesy" within the DGK since 2020.

The institute's main tasks in education focus on geodetic and industrial measurement techniques, kinematic positioning and multi-sensor systems, statistics and error theory, engineering geodesy and monitoring, GIS-based data acquisition, and transport telematics. Here, IIGS is responsible for the above-mentioned fields within the curricula of "Geodesy and Geoinformatics" (Master and Bachelor in German) and for "GEOENGINE" (Master for Geomatics Engineering in English). In addition, the IIGS provides several courses in German for the curricula of "Aerospace Engineering" (Bachelor and Master), "Civil Engineering" (Bachelor and Master), "Transport Engineering" (Bachelor and Master) and "Technique and Economy of Real Estate" (Bachelor). Furthermore, lectures are given in English to students within the Master course "Infrastructure Planning". Finally, eLearning modules are applied in different curricula.

The "Integrative Computational Design and Construction for Architecture" (IntCDC) cluster, for which the University of Stuttgart had submitted a funding application as part of the excellence strategy to strengthen cutting-edge research in Germany, was awarded funding in 2018 for the next seven years. The cluster IntCDC aims to harness the full potential of digital technologies in order to rethink design and construction, and enable ground breaking innovations for the building sector through a systematic, holistic and integrative computational approach. As a member of the cluster (IntCDC), the institute's research in the field of new construction methods is intensified in cooperation with architects, civil engineers, computer scientists, production engineers, and other scientists from various research institutions within and outside the University of Stuttgart.

The current research and project work of the institute is expressed in the course contents, thus always presenting the actual state-of-the-art to the students. As a benefit of this, student research projects and theses are often implemented in close cooperation with the industry and external research partners. The main research focuses on kinematic and static positioning, analysis of engineering surveying processes and construction processes, machine guidance, monitoring, transport and aviation telematics, process and quality modeling. The daily work is characterized by intensive co-operation with other engineering disciplines, especially with traffic engineering, civil engineering, architecture, and aerospace engineering.

This year was marked by the corona pandemic in research and teaching. In research, almost all face-to-face lectures were cancelled and in teaching, lectures were held digitally. Laboratories and exercises were also carried out digitally, but some exercises were also conducted in presence.

Research and Development

Precise Seamless 6-DoF Positioning for Georeferenced Assembly Control

The research project (RP) 16 "Robotic Assembler" is part of the research network II "Longspan Buildings" within the cluster of excellence "Integrative Computational Design and Construction for Architecture (IntCDC)" funded by the Deutsche Forschungsgemeinschaft (DFG). The cooperating disciplines within the RP are Control Engineering and Haptic Intelligence.

Gefördert durch DFG Deutsche Forschungsgemeinschaft

IntCDC CLUSTER OF EXCELLENCE

The overarching task of RP16 is the automated or semi-automated collaboration between a tower crane and a mini-crane. The mini-crane contributes to the assembly process of long span buildings. It is controlled (semi-) automatically. The boom is equipped with a universal manipulator, to which different tools can be attached, as e.g. a gripper with a haptic interface for human/machine collaboration. The IIGS contributes to the project by providing the 6-DoF pose (position and orientation) of the mini-crane or its selected components, such as the boom, through the use of a robotic total station (RTS) network. Further aspects are the investigation of optimal data fusion algorithms, e.g. Gauss-Markov-Model (GMM), Gauss-Helmert-Model (GHM), Extended Kalman Filter (EKF), Unscented Kalman Filter (UKF) and the optimization of geometric network configuration from the point of view of network quality characteristics. Two different configurations for the pose determination have been realized and investigated so far. In the first one, the RTS-network is used to determine the position. An additional inertial measurement unit (IMU) provides the orientations, in order to complement the pose. In the second configuration, the position is determined by the RTS-network, the RTS measurements, however, are also used to determine two of the three orientation angles. The third angle is still provided by the IMU. For this purpose, the mini-crane is equipped with two prisms, i.e. with two RTS tracking and measuring prism No. 1 and the remaining two RTS tracking and measuring prism No. 2. The configurations are depicted in Figure 1.

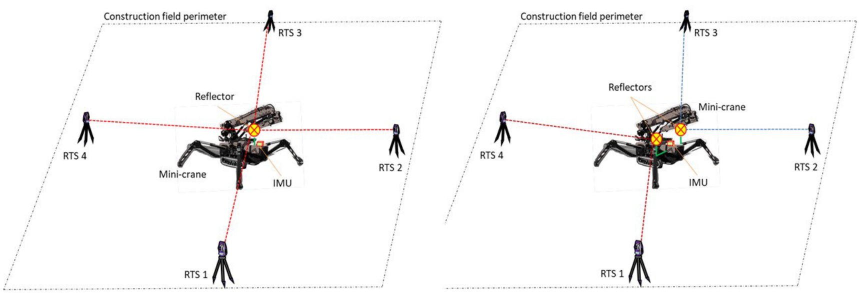

Figure 1: Left - configuration A; right - configuration B (modified from Jekko 2020).

These preliminary considerations led to the design of the deterministic model where the vector of observations, the state vector, consisting of the pose as well as the functional and the stochastic model could be defined and established. For the pose adjustment the GMM has been applied. Other approaches (GHM, EKF) are imaginable and will be introduced in the future. Regarding the network quality characteristics, the accuracy of position and orientation is derived from the covariance matrix of the adjusted state vector. For the reliability aspect the redundancy, the minimal detectable error and its impact on the parameter vector have been evaluated. The following tables show some exemplary results, obtained from simulations.

Accuracy

Configuration A	Configuration B	
$\sigma_{xyz}^{avg} = \mathbf{0.0024}\ \boldsymbol{m}$	$\sigma_{xyz}^{avg} = \mathbf{0.0033}\ \boldsymbol{m}$ (RTSs 1+4)	Position accuracy
	$\sigma_{xyz}^{avg} = \mathbf{0.0033}\ \boldsymbol{m}$ (RTSs 2+3)	

Configuration B		
Roll angle	Yaw/heading angle	Accuracy of 2 orientation angles, obtained from RTS-network
$\sigma_{\phi}^{avg} = \mathbf{0.080}°$	$\sigma_{\psi}^{avg} = \mathbf{0.076}°$	

Reliability

Impacts of the minimal detectable error on positions for different observations (values in mm)

Observation	s_1	h_1	v_1	s_2	h_2	v_2	s_3	h_3	v_3	s_4	h_4	v_4
$\nabla_{xi}^{quadsum}$	1.28	0.46	0.83	1.26	0.42	0.63	1.32	0.53	0.76	1.23	0.42	0.62

Impacts of the minimal detectable error on orientations for different observations (values in millidegrees)

Observation	s_1	h_2	v_1	s_4	h_4	v_4	s_2	h_2	v_2	s_3	h_3	v_3
∇_{ϕ}	31.73	1.56	41.38	21.40	1.46	29.71	22.68	1.32	30.85	27.44	1.89	37.3
∇_{ψ}	48.66	22.19	6.82	30.88	20.39	6.18	28.30	21.33	5.94	54.32	24.85	5.44

As an interim result, it can be stated that the average effects of the minimum detectable error on the parameters are below the position accuracy.

Supported by the Deutsche Forschungsgemeinschaft (DFG, German Research Foundation) under Germany's Excellence Strategy - EXC 2120/1 - 390831618.

Holistic Quality Model for IntCDC Building Systems

Within the framework of the Cluster of Excellence IntCDC, this project in cooperation with the Institute of Acoustics and Building Physics (IABP) and the Institute of Social Sciences (SOWI), deals with the development of a Holistic Quality Model (HQM). For this purpose, a concept was developed in which the social, environmental and technical quality requirements are first defined. Based on this concept, the quality characteristics, parameters and criteria are determined, and the interrelations between them are defined. The evaluation and assessment of the quality will be carried out at defined control and decision points in the co-design construction process (Figure 2).

Gefördert durch DFG Deutsche Forschungsgemeinschaft

IntCDC CLUSTER OF EXCELLENCE

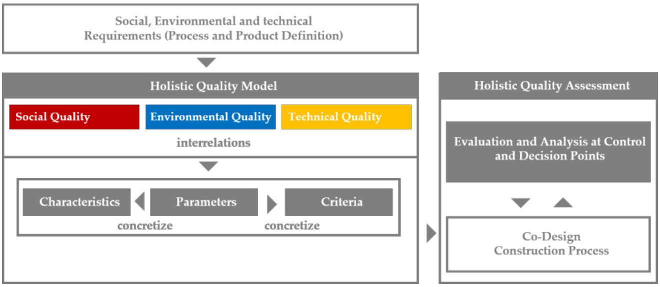

Figure 2: Quality assurance concept for the Co-Design construction process.

In contrast to the linear construction process, in which the steps of construction with definition, planning, execution, use and end-of-life are passed through linearly, these are no longer passed through linearly in co-design (Figure 3). This means that by performing a quality assessment in the planning phase at important decision points, a predicted quality assessment can serve as a decision-making aid for further planning and execution.

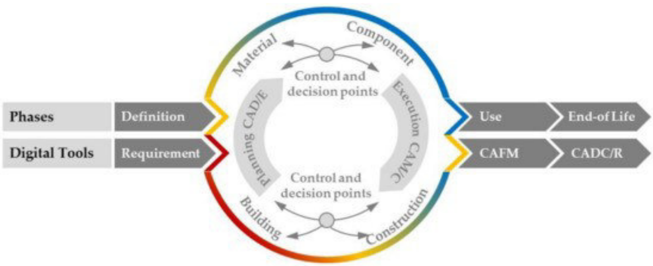

Figure 3: Holistic quality assessment in the Co-Design construction process.

Supported by the Deutsche Forschungsgemeinschaft (DFG, German Research Foundation) under Germany's Excellence Strategy - EXC 2120/1 - 390831618.

Monitoring of the Production Process of Graded Concrete Components by means of Terrestrial Laser Scanning

Accepting the ecological necessity of a drastic reduction of resource consumption and greenhouse gas emissions in the building industry, the Institute for Lightweight Structures and Conceptual Design (ILEK) at the University of Stuttgart is developing graded concrete components with integrated concrete hollow spheres. These components weigh only a fraction of the usual conventional components for the same performance. Throughout the production process of a component, the positions of the hollow spheres and the level of the fresh concrete have to be monitored with high accuracy and almost in real-time, in order to guarantee the quality and structural performance of the component. In this study, effective solutions of multiple sphere detection and concrete surface modeling based on the technology of terrestrial laser scanning (TLS) during the casting process are developed and implemented. A complete monitoring concept is presented to acquire the point cloud data quickly and with high quality. The data processing method for multiple sphere segmentation based on the efficient combination of region growing and RANSAC algorithms shows great performance in terms of computational efficiency and robustness.

The feasibility and reliability of the proposed methods are verified and evaluated by an experiment to monitor the production of an exemplary meso-graded concrete component (as shown in Figure 4). During the production process of the component in this experiment, all hollow spheres were detected and estimated in a few seconds with submillimeter accuracy. Future work includes investigating the quantitative relationship between sphere size and parameter tuning for sphere segmentation. In addition, the spatial correlations of the point cloud can be taken into account when building the stochastic model for sphere fitting. Thus optimized parallel processing of multiple-sphere detection is possible for production monitoring of large-scale graded concrete components with hundreds of hollow spheres.

(a) (b) (c)

Figure 4: The process of automatic detection of multiple hollow spheres in the production of a meso-graded concrete component.

Quality Control of the Manufacturing Geometry for Fiber Components

Laser scanning measurements were carried out as part of the investigation into the manufacturing accuracy of fiber components (Figure 5). On the one hand, a column of the BUGA pavilion and various components of a biennale installation in 2021 were scanned. The difficulty here was the evaluation of the measurement results, since no classic CAD model was available for comparison and the individual point measurements had to be assigned to the line model from the design in order to obtain information about the geometry of the individual lines of the element.

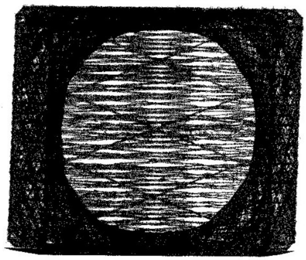

Figure 5: Scanned Fiber Component.

Collaborative Scanner Test and Calibration on the Bonn Reference Wall

Within the framework of the project "Collaborative scanner test and calibration on the Bonn reference wall" (COLLECTOR) carried out by the Gesellschaft zur Kalibrierung Geodätischer Messmittel (GKGM) a comparison of various Laser scanners from different universities will be made. The IIGS participates in this project with four Laser scanners (Leica HDS7000, Leica BLK, Trimble X7, Riegl 2000V). All four scanners are used to survey the exterior of the Bonn wall (Figure 6 and Figure 7).

Figure 6: Measurement setup at Bonn reference wall.

Measurements are made in two faces from three instrument points. The aim is to estimate the wall parameters from all scanner measurements and compare the results with other universities. In addition, calibration measurements were performed with three of these scanners in the calibration area in Bonn. In order to obtain comparable results all participants have to use a provided software for the evaluation.

Figure 7: Scanned wall from Trimble X7.

Monitoring of the Urbach tower

Similar to the previous year, the wooden tower of ICD in Urbach is to be monitored at least twice a year. To achieve a detailed look at possible deformations, the tower was scanned using the HDS7000 from Leica. In addition, the tower was scanned several other times, bringing the total number of scans to four during the year. The working process was disturbed, since reference points in the surrounding area, which helped to compare scans (deformation analysis), were removed. No major deformations were detected during the year (Figure 8). The tower will continue to be monitored over the next 3 - 4 years.

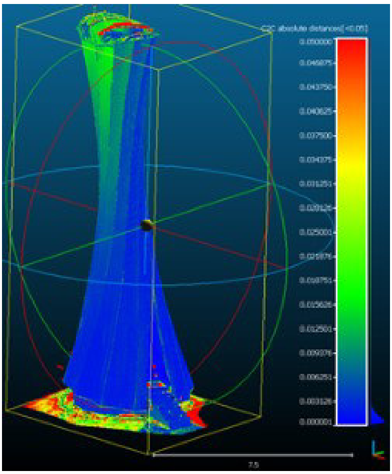

Figure 8: Deformation analysis of a two epoch measurement.

Perceived Space Representation using Brain Activity Analysis, Eye-Tracking and Terrestrial Laser Scanning (Brain TLS)

Is the human a measurement instrument (Figure 9)? Within this RISC (Research Seed Capital - Blue Skies Research) project, it is considered that the brain activity and eye movement analysis of a person in combination with a space-calibration method can be used to represent the perceived space.

Humans describe reality with the help of vertical perception and pre-knowledge. Nowadays, brain activity analysis may be done through non-invasive methods. Most studies in the field of neuroscience are related to extracting information after observing the state of the brain. Eye-Tracking, on the other side, is used to analyze fixations and saccades by recording pupil movements with external cameras. This can be done for a multitude of purposes, but this project focuses on the gaze positions in a defined area. The question arises if the signals captured with a Brain Computer Interface (BCI) combined with eye-tracking information and corrected by an existing 3D model of the observed space can be used to create a digital representation of the same space.

Figure 9: Is the human a measurement instrument?

The scale and geometry of the perceived space are firstly defined with the help of a 3D terrestrial laser scanner (TLS). The implied methods and experiments aim at establishing a connection between instrument-measured space and human-perceived space. Defining geometric relationships between the observer (person) - observed objects and finding a correlation of the geometric attributes with the brain activity and eye-tracking data are the main goals of this project. If these goals are achieved, an innovative measurement method may be developed and a better insight into how the human brain perceives the surrounding space may be gained.

Integrated space-time modeling based on correlated measurements for the determination of survey configurations and the description of deformation processes (IMKAD II)

Gefördert durch DFG Deutsche Forschungsgemeinschaft

This DFG (Deutsche Forschungsgemeinschaft) project foresees the establishment of a stochastic model for scans acquired with high-end Terrestrial Laser Scanners (TLS). The resulting stochastic model is based on the elementary error (EE) theory and describes uncertainties and correlations in form of a synthetic variance-covariance matrix (VCM). With this information, B-Spline surfaces are estimated for each epoch according to individual variances and covariances of the point cloud.

As explained in previous reports, several measurement campaigns are necessary during the whole project. In July 2020, the first measurements of the "Urbach Tower" were completed. This wooden tower was erected for the "Remstal Gartenschau 2019" and is perfectly suitable for B-Spline modeling. The outer shell is made out of double curved self-forming wooden panels.

Shortly after, in August 2020, the second measurement campaign of the Kops water dam in Austria was successfully completed. Specifically, for this object, a new approach for computing the VCM is introduced (Kerekes & Schwieger, 2020). Environmental parameters like air temperature, air pressure, and vertical temperature gradient (VTG) are treated as stochastic correlating influences. As known from trigonometric leveling and EDM measurements, distances and zenith angles are mostly affected by air temperature and VTG. This effect has recently gained much attention in the scientific TLS community. The overall contribution of environmental parameters (Atmospheric EE) on single points using the EE theory can be seen in Figure 10. Points that are closer to the ground are strongly affected by the intense variations in air temperature and VGT (especially in summer), whilst points on the dam crown are less influenced by the variations in the lower VGT layers.

Statistical investigation of Boehm's algorithm for B-Spline Modeling

In the context of forming rectangular grid structures as the basis of a uniform control grid for NURBS (non-uniform rational B-Splines) surface generation, two node insertion algorithms are examined in more detail. These are on the one hand Boehm's algorithm and on the other hand Oslo algorithm. While Boehm's algorithm inserts one node at a time in one computation pass, Oslo algorithm inserts several nodes in one pass, but this requires the formation of n +1 matrices where n corresponds to the degree of curvature. A comparison of the computation times of both algorithms has shown that Boehm's algorithm has a shorter computation time compared to the version of the Oslo algorithm used here. Therefore, Boehm's algorithm will be used for the filling of control points for NURBS curves and surfaces.

Apart from the mathematical consideration of Boehm's algorithm, which shows that the shape of the NURBS curve or surface is identical before and after node insertion, this statement

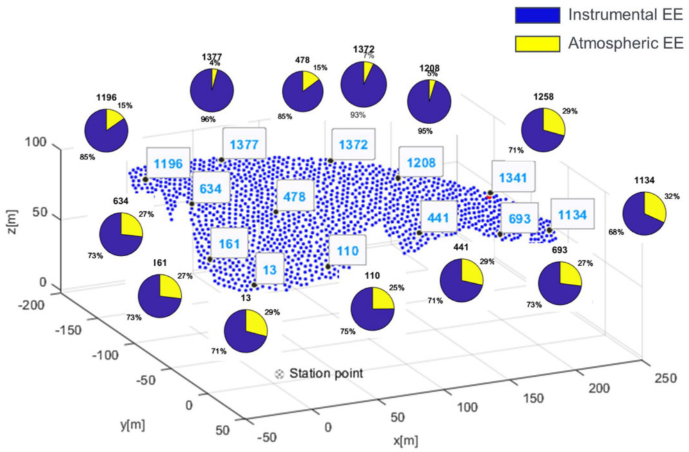

Figure 10: Contribution to the error budget of individual points according to the EE theory.

shall be verified by means of a statistical procedure. By covariance propagation the standard deviation of the newly formed control points and thus the influence of Boehm's algorithm can be determined. For the standard deviation of the old control points before applying Boehm's algorithm, a variance of 1 mm^2 is assumed in the first instance.

Figure 11 shows a third degree B-spline curve and its control polygon in gray before applying Boehm's algorithm, and in black after its execution. The two newly formed control points q_4 and q_5 have a standard deviation of 0.75 mm instead of a value of 1 mm. The standard deviations of the two new control points are thus 0.25 mm smaller than the original standard deviation. When calculating the standard deviations of the new control points of a NURBS surface, a similar behavior appears. Depending on how many control points have to be inserted into a polygon using Boehm's algorithm, the standard deviation decreases step by step.

Automated gap and flush measurement between car parts assisted by a high flexible and accurate robot system

This research is the result of a partnership between the Institute of Engineering Geodesy (IIGS) at the University of Stuttgart and the Tec-Fabric at the Mercedes-Benz AG plant in Sindelfingen. In general, the measuring tool is attached to a lightweight robot (LBR), which is mounted on a driverless platform KMP. Gap and flush measurements between two structural car components are part of the quality assurance process in Daimler AG's production. Measurement data is collected in three manufacturing phases during the car body construction, car varnishing and body assembly. As a result of observing the gap and flush values throughout the entire process, functional as well as customer-specific requirements can be guaranteed.

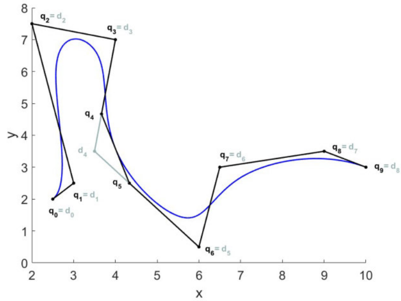

Figure 11: Third degree B-spline curve with control polygon before and after application of Boehm's algorithm.

At the assembly line, full automatic gap measuring installations or hand-held instruments measure gap and flush values. Car bodies, in which errors are identified during the measurement process, will be channeled out of the production line. Adjacent to the production line, two employees process the rework and repeat the required quality measurements in order to assure that they comply with the quality targets. Once the required corrections are successfully executed, the car is channeled back into the production line. The gap measurement with mobile devices (SME, Figure 12), realized with a lightweight robot in human-robot interaction (MRK), enhances the automation and the flexibility within the production. The mobile units today are mounted at a fixed position in the assembly line, but can easily be moved to another location. In the future, systems like the SME are supposed to replace the static measurement cells. Likewise, the measurement outside the production line is supposed to be scalable and autonomous. In order to accomplish this, two of the main components from the SME are used: measurement devices and the lightweight robot (LBR) are mounted on a driverless platform (KMP). The aim of this research was to develop a measuring system, which is precise enough to satisfy the quality requirements of a Mercedes-Benz car. We were able to patent the system mentioned above this year.

Figure 12: Mobile device for gap measurement.

Multi-Sensor Fusion for Environment Perception

For autonomous vehicles and automated safety functions, a comprehensive environment perception is necessary. This applies in particular for urban situations with multiple dynamic objects, like in many of the TransSec use cases. Different Sensor systems are able to detect objects with different accuracies in spatial position and classification. Lidar sensors offer high spatial precision with low classification accuracy, while cameras show great classification performance, but lack in spatial accuracy. To overcome the uncertainties of both measurement principles, object detections of Lidar and Camera are fused on object level. The fusion is done during the data assignment step of a multi-object tracker. Different three-dimensional geometrical shapes, like oriented bounding boxes or point cloud segments can be incorporated through the usage of turning functions for spatial association (Figure 13). The multi-object tracker is based on an interacting multiple model with unscented Kalman filter. This allows a motion model based trajectory prediction with a time horizon of 1 s for all dynamic objects. GNSS and map data allow an extension of this time horizon by making long time predictions based on the provided street network. Each dynamic object is assigned to a street segment under the assumption that the object will follow the road trajectory. Next, a combined trajectory of the motion model prediction and the road trajectory prediction is calculated with a high weight on the motion model for short term predictions and a high weight on the road trajectory prediction for long term prediction.

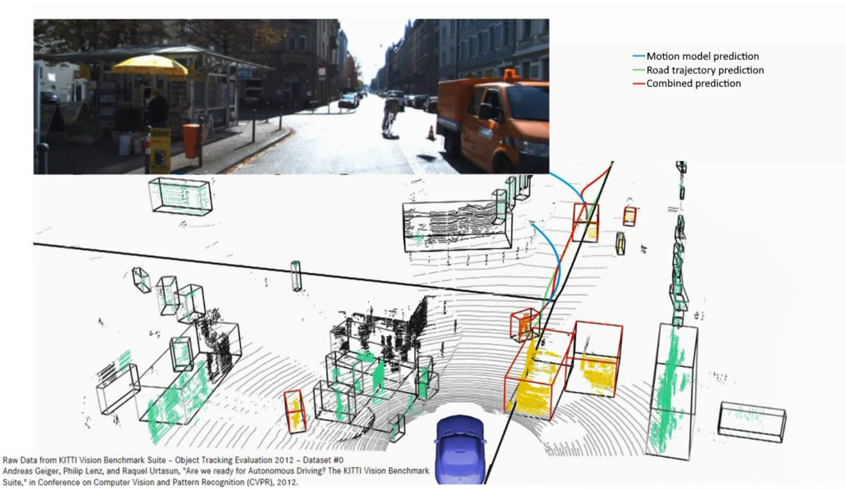

Figure 13: Multi-Sensor Fusion for Environment Perception.

3D Lidar based road curb detection with adapted geometry constrains

A 3D Lidar based road detection is usually realized by detecting distinctive road boundaries such as road curbs. An example for road geometry and road curb measured by a 3D Lidar sensor is shown in the figures below (Figure 14).

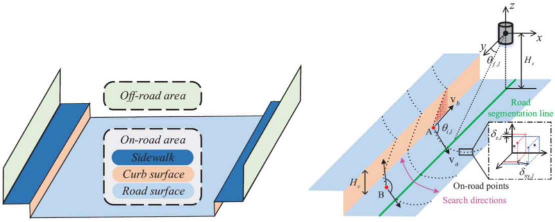

Figure 14: left: road geometry description; right: curb scenario description. (Source: Zhang, Yihuan, et al. "Road-segmentation-based curb detection method for self-driving via a 3D-LiDAR sensor". IEEE transactions on intelligent transportation systems 19.12 (2018): 3981-3991.

The state-of-the-art 3D Lidar based curb detection algorithm utilizes the spatial relation of adjacent laser points for curb candidate searching, and accomplishes the eventual detection task by filtering out noisy curb candidates with an estimated road shape. A typical algorithm pipeline mainly includes the following steps:

- Data pre-processing: as the first step the input 3D point cloud will be rectified through sensor calibration and vehicle motion compensation, then a ground plane will be fitted to the input point cloud in order to segment all 3D points as either on-road or off-road.
- Road shape recognition: the purpose of this step is to estimate the road shape (the rough centerline of the road), as this will be required to filter out noisy curb candidates from the detection result.
- Curb candidate detection: each laser ring is treated as an independent processing unit, and several filtering criteria are then applied to detect all curb candidates within a laser ring:
  - a) horizontal distance threshold: $\delta_{xy,l} = H_s \cdot \cot\theta_{f,l} \cdot \frac{\pi\theta_a}{180}$, where: H_s is sensor height, $\theta_{f,l}$ is the vertical pointing angle of lth laser ring, and θ_a the horizontal angular resolution of the Lidar.
  - b) vertical distance threshold: $\delta_{z,l} = \delta_{xy,l} \cdot \sin\theta_{f,l}$
  - c) horizontal adjacent angle: $\theta_{I,l} = \cos^{-1}\frac{v_a \cdot v_b}{|v_a| \cdot |v_b|}$, where v_a and v_b represents adjacent horizontal vectors in both scan- and counter-scan directions. Usually a constant threshold is set for this calculated horizontal adjacent angle, e.g. 150°.

Notably, the assumption behind these calculated thresholds is that the projected geometry of each laser ring onto ground is a perfect circle. However, depending on factors such as sensor installation, road slope and vehicle dynamics, the projected geometry of a particular laser ring may vary between circle, ellipse, parabola and hyperbola. Figure 15 demonstrates this change caused by the relative angle between sensor horizontal plane (X-O-Y) and the ground plane (in green).

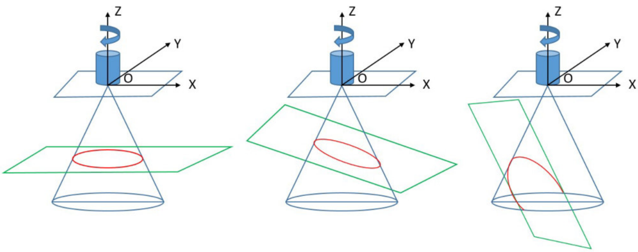

Figure 15: The projected geometry (in red) of a laser ring onto a ground plane (in green). From left to right the projected geometry: circle, ellipse and parabola.

Therefore, an optimization has been conducted with respect to a state-of-the-art algorithm, where the adapted geometry is used for calculating these thresholds. The performance of this optimized detection algorithm was primarily evaluated on a public 3D Lidar dataset, and the results are summarized as follow (Table 1).

Table 1: Performance evaluation of the optimized algorithm w.r.t. the original algorithm.

Algorithm	Optimized		Original (Zhang, et al. 2018)	
Road type	Straight	Curve	Straight	Curve
Precision	0.8773	0.8686	0.8230	0.8764
Recall	0.7801	0.8701	0.7716	0.8227
F1	0.8247	0.8688	0.7597	0.8483

It is notable that, for straight road type, the optimized algorithm surpasses the state-of-the-art algorithm in all three metrics. However, as can be seen from Figure 16, some of the detected curb points are actually correct but the corresponding ground truth are missing in this dataset, and this could result in a lower detection precision. In future, the developed algorithm will be further optimized and evaluated in a larger open dataset, e.g. Semantic KITTI dataset.

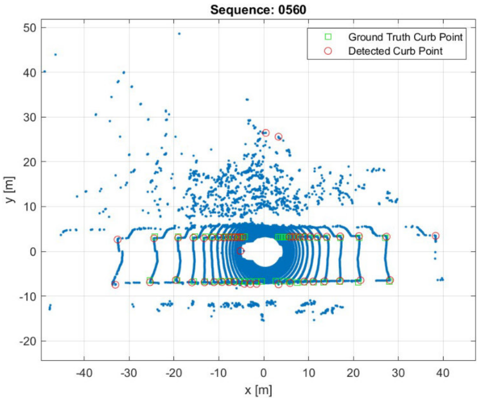

Figure 16: One example of the detection result from the optimized algorithm.

Ghosthunter II - Telematics System against Ghost Drivers using GNSS

The aim of the Ghosthunter II research project is to develop a detection system to extend current car navigation systems detecting ghost drivers on freeways and their ramps and warning both the ghost drivers themselves and other road users. This project is carried out in cooperation with the Institute of Space Technology and Space Applications at the University of the Federal Armed Forces Munich and the company NavCert.

Supported by:

Federal Ministry for Economic Affairs and Energy

on the basis of a decision by the German Bundestag

For this purpose, an android-based app was developed as a demonstrator. The app is used to detect wrong-way drivers and to send a warning via mobile radio to a server. This server distributes the warning to all other app users. The developed app, that is currently providing a warning to a wrong-way driver, is shown in Figure 17.

As mentioned above, a central goal is to detect wrong-way drivers reliably and as early as possible on freeway ramps. However, previous approaches and implementations could only perform this detection if there was a constructional separation of the lanes. In order to circumvent this limitation and to be able to start the detection earlier, the previous algorithms were further developed in this direction. The idea here is to use statistical tests to detect whether the vehicle is significantly to the left or right of the centerline of the lane. This statement is made based on the standard deviation of the vehicle position and the map as well as the current road geometry.

The research project Ghosthunter II is granted by the German Federal Ministry of Economic Affairs and Energy (BMWi) and the German Aerospace Center (DLR) under grant number 50 NA 1802.

Figure 17: Ghosthunter app for wrong-way driver detection.

TransSec - Autonomous Emergency Maneuvering and Movement Monitoring for Road Transport Security

The European Project TransSec (Autonomous Emergency Maneuvering and Movement Monitoring for Road Transport Security) is funded by the European Commission under the Horizon H2020 program for three years. This project was launched in February 2018 and aims to design and implement a built-in intelligent safety system to prevent trucks and transports of goods from being misused for illegal purposes such as terrorist attacks. The Institute of Engineering Geodesy (IIGS) at the University of Stuttgart is one of the five partners involved in the TransSec project. The project concluded with an online event in January 2021. The deliverables were all defined within 2020.

European Commission

European Global Navigation Satellite Systems Agency

One task of the IIGS was to obtain the precise positioning of the trucks by integrating data from GNSS and other additional sensors such as IMU. IIGS focuses on an error-state Kalman-filter with strapdown algorithm in the positioning module. The other task of the IIGS was to design and implement a map-aiding approach that takes into account on-road and especially off-road scenarios as well as wrong-way driver detection for trucks. The final parts of these two tasks will be described in the following text.

TransSec - Positioning Module

For the research project TransSec the IIGS created a positioning module together with OHB Digital Solutions GmbH (formerly TeleConsult Austria), who is one of the project partners. Since the GNSS availability decreases and even complete outages occur in urban city canyons or other obstructed areas like tunnels, we designed an integrated multi-sensor positioning system. The sensor data fusion uses GNSS and inertial measurement unit (IMU) inputs and is performed by using an error-state Kalman filter. In the last year of the project the positioning module was tested in real case scenarios. Here, the results of urban and sub-urban test drives with a length of 13 km are presented. For the test drives we used a u-blox C099-F9P application board with a ZED-F9P chip in combination with an XSens Mti 100 IMU, generating stand-alone code solutions as input for the filter. A Leica GS15 receiver with SAPOS-RTK correction signals was used as reference. The comparison between the filter result and the reference situation results in an RMS of 1.1 m. The accuracy was not significantly improved over the GNSS to reference comparison, but the availability was considerably improved. In addition, the solution was smoother and the difference between filter solution and GNSS stand-alone solution was 0.46 m RMS, indicating the difference. The challenge in tunnels remains because the low-cost IMU shows drift effects (e.g., up to a few deca m deviation). Figure 18 shows blue dots for the reference solution and a green line for the filtered solution. The figure shows an obvious alignment of the two trajectories and the tunnel challenge.

Figure 18: Tunnel drive (green: 100 Hz filter solution, blue: 10 Hz reference solution).

TransSec - Map-Aiding

Within this project, the Institute of Engineering Geodesy (IIGS) at the University of Stuttgart designed and implemented a map-aiding approach that considers on-road and particularly off-road scenarios for trucks. This includes the identification of the driven lane. Figure 19 shows the geometrical relationship for a road with four lanes including the rough knowledge about the lane width as well as the geometrical on-road/off-road decision. Recent developments include statistical testing and error probabilities for on-road/off-road decision making as well as for correct/opposite lane driving. For these decisions, the accuracy of the position, either determined by GNSS or by a sensor fusion such as the aforementioned error-state Kalman-filter, as well as the map accuracy are taken into account. For the latter, one has to rely on assumptions about e.g. the width of a lane. It is assumed that these assumptions will be filled with real data in the future. In this case, the algorithm can be adopted without problems to newly available stochastic models.

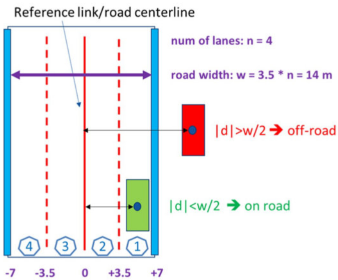

Figure 19: On-/Off-Road Decision ad lane detection.

Dynamic Location Referencing: Probability and Fuzzy Logic Based Decision Systems

To share geo-objects between digital maps, location referencing is a well-known methodology typically used to exchange traffic information such as traffic jams, road works, etc. In very many cases, there is no common database between the systems (maps) to be exchanged. For this purpose, dynamic (on-the-fly) methods are developed to exchange Location References (LR, geo-objects based on digital maps) between different maps in such special cases where no common databases and/or common structures are available.

In general, location referencing methods follow a one-dimensional three-step process of encoding the LR in the sender system, transmitting it, and decoding it in the receiver system without iterations and typically limited bandwidth. Given the fact that there are no dedicated links/common data structures between maps, the key issue in Dynamic Location Referencing is to find the correct LR in the target map that corresponds to the LR in the source map (see Figure 20).

To accomplish this, deterministic algorithms are defined and implemented in almost all methods.

Following the uncertainty in matching procedures for geodata, uncertainty-based decision systems are explored. Thus, a probability-based and a fuzzy-based approach have been specified and studied in detail as two different uncertainty-based concepts. For both, a set of decision criteria (geometric, topological, syntactic and semantic) was defined and the decision algorithms were formulated. Both approaches were implemented and analyzed in an

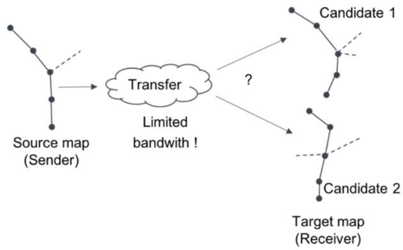

Figure 20: Identification of Location Reference.

evaluation system. As published in the conference proceedings of the LBS Conference 2019 in Vienna, the probability-based and fuzzy-based approaches show similar results with an average hit rate up to 90 % and improve the results of a comparable deterministic approach (OpenLR) by 12 percentage points on average.

As stated in the last report, further aspects were discussed to validate the previous results as well as to extend the research approach. This is still in progress and will be finalized in the course of this year.

Multipath effects influence on the position

In order to investigate the influence of multipath effects on the position, real test drives were completed and the data was analyzed. To understand the critical situations for an urban roadway, a representative situation was considered: tall buildings. The reference coordinates of the test vehicle were obtained using iTraceRT F402-E. These were compared to the GNSS position obtained using DGNSS based on the pseudo-range.

Buildings

The main challenge related to multipath in the urban environment is represented by the tall buildings that are present along the roadway. An example of such a situation is illustrated in Figure 21. On the left side of the figure, the GNSS position based on pseudo ranges which drifts due to multipath effects is shown in red. The car reference position is shown in green. A deviation from the car reference trajectory occurs along the left building between the intersections. This is probably the effect of signal reflections, due to the tall building. The vehicle velocity is shown along with the satellite availability on the right side of Figure 21. It is shown that the number of satellites used varies between 7 and 10. Due to the proximity of the vehicle to the tall building on the left, the satellites on the right suffer strong reflections, therefore there is an increased signal time-of-arrival.

The multipath delay caused by such a situation is short due to the proximity of the vehicle to the building. At the same time, the satellites on the left side are obscured and cannot compensate for the multipath error. Consequently, the position drift occurs in the opposite direction of the building.

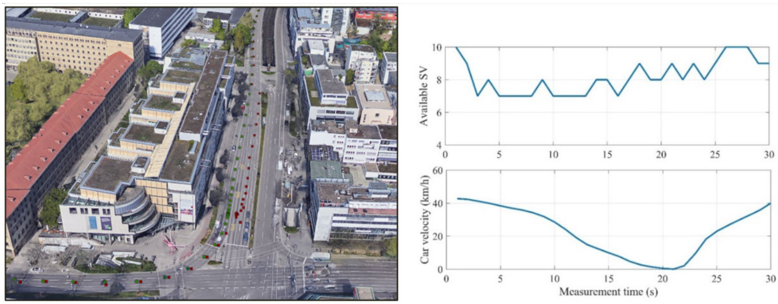

Figure 21: Position drift due to multipath reflections on an urban highway scenario, satellite availability and vehicle velocity. Reference position (green) and position changed by multipath (red) are shown based on Google Earth®.

Figure 22 shows the deviation in latitude, longitude, and height, as well as the RMS error for the investigated segment. The errors in latitude and longitude increase with about 4 meters as the vehicle begins to travel parallel to the building. The height is the most affected with a value around 10 meters. Overall, the RMS increases from 3.5 meters up to a maximum of 16.9 meters.

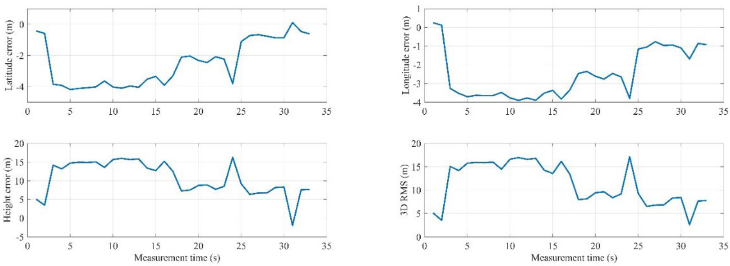

Figure 22: Deviation of the ellipsoidal 3D coordinates and RMS error in the multipath environment determined by the tall building.

PhD Seminar

The 10th PhD Seminar of the Engineering Geodesy Section of the DGK was organized by the IIGS and had to be realized in a fully digital format. More than 50 participants from Austria, Switzerland, Croatia and Germany attended the event on October 22 and 23, 2020. Ten presentations were followed by lively discussions. Digital meetings were possible in so-called virtual subspaces of the video conferencing tool. This worked surprisingly well. The only thing missing was the social event in the evening, which could not be replaced by digital means.

Publications

Refereed Publications

Balangé, L.; Zhang, L.; Schwieger, V. (2021): First Step Towards the Technical Quality Concept for Integrative Computational Design and Construction. In: Kopáčik, A.; Kyrinovič, P.; Erdélyi, J.; Paar, R.; Marendić, A. (eds) Contributions to International Conferences on Engineering Surveying. Springer Proceedings in Earth and Environmental Sciences. Springer, Cham. https://doi.org/10.1007/978-3-030-51953-7_10

Kerekes, G.; Schwieger, V. (2021): Determining Variance-Covariance Matrices for Terrestrial Laser Scans: A Case Study of the Arch Dam Kops. In: Kopáčik A., Kyrinovič P., Erdélyi J., Paar R., Marendić A. (eds) Contributions to International Conferences on Engineering Surveying. Springer Proceedings in Earth and Environmental Sciences. Springer, Cham. https://doi.org/10.1007/978-3-030-51953-7_5

Kerekes, G.; Schwieger, V. (2020): Elementary Error Model Applied to Terrestrial Laser Scanning Measurements: Study Case Arch Dam Kops. Mathematics 2020, Vol. 8(4), 593.

Lerke, O.; Schwieger, V. (2020): Genauigkeitsanalyse der automatischen Werkzeugsteuerung eines Laderaupenmodells. In: Ingenieurvermessung 20, Beitragsheft zum 19. Internationalen Ingenieurvermessungskurs München 2020, Thomas A. Wunderlich (Hrsg.). Wichmann, VDE Verlag GmbH, Berlin, Offenbach. ISBN 978-3-87907-672-7.

Luz, P.; Metzner, M.; Schwieger, V. (2020): Development of a new lane-precise map matching algorithm using GNSS considering road connectivity. Online proceedings of Virtual ITS European Congress, 9-10.11.2020

Schwieger, V.; Kerekes, G.; Lerke, O. (2020): Image-Based Target Detection and Tracking Using Image-Assisted Robotic Total Stations. In: Sergiyenko O., Flores-Fuentes W., Mercorelli P. (eds) Machine Vision and Navigation.

Zhang, L.; Balangé, L.; Braun K.; Di Bari, R.; Horn, R., Hos, D.; Kropp, C.; Leistner, P.; Schwieger, V. (2020): Quality as Driver for Sustainable Construction - Holistic Quality Model and Assessment. Sustainability 2020, 12(19), 7847; doi: 10.3390/su12197847.

Zhang, L.; Schwieger, V. (2020): Reducing Multipath Effect of Low-Cost GNSS Receivers for Monitoring by Considering Temporal Correlations. Journal of Applied Geodesy, Band 14, Heft 2, ISSN (Online) 1862-9024, ISSN (Print) 1862-9016, doi: 10.1515/jag-2019-0059.

Non-Refereed Publications

Scheider, A.; Schwieger, V.; Brüggemann, T. (2020): Entwicklung eines Multisensorsystems zur Georeferenzierung von hydrographischen Messdaten auf Binnengewässern. In: Ingenieurvermessung 20, Beitragsheft zum 19. Internationalen Ingenieurvermessungskurs München 2020, Thomas A. Wunderlich (Hrsg.). Wichmann, VDE Verlag GmbH, Berlin, Offenbach. ISBN 978-3-87907-672-7.

Wachsmuth, M.; Koppert, A.; Zhang, L.; Schwieger, V. (2020): Development of an error-state Kalman Filter for Emergency Maneuvering of Trucks. European Navigation Conference. 23.-24.11.2020.

Monographs, books and book chapters

Kuhlmann, H.; Holst C.; Zhang, L.; Schwieger, V. (2020): Ingenieurgeodasie. In: Kummer, K.; Kötter, T.; Kutterer, H.; Ostrau, S. (Hrsg.): Das deutsche Vermessungs- und Geoinformationswesen 2020. Wichmann Verlag, Berlin.

Presentations

Balangé, L., Di Bari, R., Deniz Hos, P.: Holistic Quality Model for IntCDC Building Systems, Status Colloquium 2020, 17.02.2020

Di Bari, R., Deniz Hos, P.: Holistic Quality Model, Status Seminar 2020, 12./13.11.2020

Lerke, O.: Project Status - Precise Seamless 6DoF Positioning for Georeferenced Assembly Control, General Meeting RP16, 28.09.2020

Lerke, O.: Research Progress - Precise Seamless 6DoF Positioning for Georeferenced Assembly Control, Status Meeting RP 2, RP 8, RP 16: RP16, 10.12.2020

Lauer, A., Lerke, O., Mohan, M., Gong, Y.: RP16 - Robotic Platform for Cyber-Physical Assembly of Long-Span Fibre-Composite Structures, Research Update on Robotic Total Station Network for Seamless 6DoF determination, 2020 IntCDC Status Colloquium Research Networks, 17.02.2020

Lauer, A., Gong, Y., Mohan, M., Javot, B., Ortenzi, V., Lerke, O.: RP16 - Research Update on Precise Seamless 6DoF Positioning for Georeferenced Assembly Control, 2020 IntCDC Status Seminar,12./13.11.2020

Schwieger, V.: Map Matching Applications. Seminar SE 3.05 "GPS/INS-Integration und Multisensor-Navigation", Carl-Cranz-Gesellschaft e.V., Oberpfaffenhofen, 21.10.2020.

Schwieger, V.: Varianzfortpflanzung und Elementarfehlermodell (am Beispiel TLS) - Möglichkeiten und Grenzen. Joint Workshop DGK - Abteilung Ingenieurgeodäsie & GKGM "Unsicherheitsmodellierung beim Einsatz komplexer Messsysteme", 21.09.2020.

Schwieger, V.: Vorstellung der Abteilung Ingenieurgeodäsie, Jahressitzung des Ausschusses Geodäsie (DGK), Bayrische Akademie der Wissenschaften, 23.11.2020.

Activities at the University and in National and International Organizations

Volker Schwieger

Dean of the Faculty of Aerospace Engineering and Geodesy, University of Stuttgart
Full member of the German Geodetic Commission (Deutsche Geodätische Kommission - DGK)
Head of the section "Engineering Geodesy" within the German Geodetic Commission (DGK)
Chief Editor of Peer Review Processes for FIG Working Weeks and Congresses
Member of the Editorial Board "Journal of Applied Geodes"
Member of the Editorial Board "Journal of Applied Engineering Science"
Member of the Editorial Board "Journal of Geodesy and Geoinformation"

Martin Metzner

Member of the NA 005-03-01 AA "Geodäsie" at the DIN German Institute for Standardization
Course Director of the MSc Program GeoEngine at the University of Stuttgart

Li Zhang

Co-Chair of the Working Group 5.6 "Cost Effective Positioning" within the FIG Commission 5 (Positioning and Measurement)
Chair of the Working Group "Quality Assurance" within the Commission 3 "Measurement Methods and Systems" of "Deutscher Verein für Vermessungswesen (DVW)"

Doctorates

Lerke, Otto: Entwicklung eines Steuerungssystems für eine Laderaupe zur Durchführung vollautomatisierter Ladeprozesse unter Einsatz bildverarbeitender Robottachymeter und adaptiver Regelung. Main reviewer: Prof. Dr.-Ing. habil. V. Schwieger, co-reviewers: Prof. Dr.-Ing. Hans Neuner, Prof. Dr. Andreas Wieser

Pham, Trung Dung: Use of Non-linearity as a Characteristic in the Selection of Filtering Algorithms in Kinematic Positioning. Main reviewer: Prof. Dr.-Ing. habil. V. Schwieger, co-reviewer: Prof. Dr.-Ing. Uwe Sörgel

Stefan Cavegn: Integrated Georeferencing for Precise Depth Map Generation Exploiting Multi-Camera Image Sequences from Mobile Mapping. Deutsche Geodätische Kommission, Reihe C, Nr. 863, München 2020. Main reviewer: Prof. Dr.-Ing. Norbert Haala, co-reviewers: Prof. Dr.-Ing. habil. Volker Schwieger, Prof. Dr. Stephan Nebiker

Master Theses

Mohammed Ismail: Integration of constraints in filters for navigation purposes (M. Wachsmuth)

Pascal Kaiser: KI-basierte und AR-gestützte Nachbearbeitung von Spalten beim Einbau von Kotflügeln (V. Schwieger)

Nian Liu: Development of a Real-Time Magnetometer Calibration Solution (V. Schwieger)

Christoph Pfeil: Qualitätsverbesserung im Hochbau gezeigt an einem Praxisbeispiel (L. Balangé)

Andreas Pfemeter: Entwicklung von Sensorsystemen zur Umfelderkennung von automatischen Türen und Klappen (O. Lerke)

Daniele Roos: Objekterkennung von Bauteilzuständen in der Rohbauphase von Hochbauprojekten mit Hilfe von künstlichen neuronalen Netzen (L. Balangé)

Mansoor Sabzali: Improving the modeling of atmospheric effects on long-range TLS measurements (G. Kerekes)

Bachelor Theses

Christine Dräger: Robuste Dienstplanung an Flughäfen (V. Schwieger)

Ivan Hybsch: Projektübergreifende Datenanalyse von Verzögerungen und Störungen in Bauprojekten durch den Einsatz von Machine Learning (M. Metzner)

Education

SS20 and WS20/21 with Lecture/Exercise/Practical Work/Seminar

Bachelor Geodesy and Geoinformatics (German)

Basic Geodetic Field Work (Wachsmuth, Kanzler)	0/0/5 days/0
Engineering Geodesy I (Schwieger, Basalla)	4/2/0/0
Engineering Geodesy II (Schwieger, Lerke)	1/1/0/0
Geodetic Measurement Techniques I (Metzner, Hausmann)	3/1/0/0
Geodetic Measurement Techniques II (Wachsmuth)	0/1/0/0
Integrated Field Work (Kerekes, Metzner)	0/0/10 days/0
Reorganisation of Rural Regions (Helfert)	1/0/0/0
Statistics and Error Theory (Schwieger, Balangé)	2/2/0/0

Master Geodesy and Geoinformatics (German)

Deformation Analysis (L. Zhang)	1/1/0/0
Industrial Metrology (Schwieger, Y. Zhang)	1/1/0/0
Land Development (Eisenmann)	1/0/0/0
Monitoring Measurements (Schwieger, Kerekes)	1/1/0/0
Terrestrial Multisensor Systems (L. Zhang, Lerke)	1/1/0/0
Transport Telematics (Metzner, Luz)	2/2/0/0

Master GeoEngine (English)

Kinematic Measurement Systems (Schwieger, Basalla)	2/2/0/0
Monitoring (Schwieger, Balangé)	1/1/0/0
Thematic Cartography (L. Zhang, Hausmann)	1/1/0/0
Transport Telematics (Metzner, Y. Zhang)	2/1/0/0
Terrestrial Multisensor Systems (L. Zhang, Lerke)	2/1/0/0

Bachelor and Master Aerospace Engineering (German)

Statistics for Aerospace Engineers (L. Zhang, Balangé, Hassan)	1/1/0/0

Master Aerospace Engineering (German)

Industrial Metrology (Schwieger, Y. Zhang)	1/1/0/0
Transport Telematics (Metzner, Luz)	2/2/0/0

Bachelor Civil Engineering (German)

Geodesy in Civil Engineering (Metzner, Hassan, Kanzler)	2/2/0/0

Master Civil Engineering (German)

Geoinformation Systems (Metzner, Luz)	2/1/0/0
Transport Telematics (Metzner, Luz)	2/1/0/0

Bachelor Technique and Economy of Real Estate (German)

Acquisition and Management of Planning Data and Statistics (Metzner, Luz, Kanzler)	2/2/0/0

Bachelor Transport Engineering (German)

Statistics (Metzner, Luz, Kanzler)	0.5/0.5/0/0
Seminar Introduction in Transport Engineering (Basalla)	0/0/0/1

Master Infrastructure Planning (English)

GIS-based Data Acquisition (L. Zhang, Y. Zhang)	1/1/0/0

Institute of Geodesy

Geschwister-Scholl-Str. 24D
D-70174 Stuttgart
Tel.: +49 711 685 83390
Fax: +49 711 685 83285
gis@gis.uni-stuttgart.de
http://www.gis.uni-stuttgart.de

Head of Institute

Prof. Dr.-Ing. Nico Sneeuw
Prof. Dr. James Foster (since 10.3)

Emeritus

em. Prof. Dr.-Ing. habil. Dr. tech. h. c. mult. Dr.-Ing. E. h. mult. Erik W. Grafarend (†08.12.2020)
Prof. Dr. sc. techn. Wolfgang Keller

Academic Staff

Dr.-Ing. Markus Antoni	Physical Geodesy, Satellite Geodesy
Dr.-Ing. Jianqing Cai	Satellite Geodesy, Adjustment Theory
Dr. Karim Douch	Physical Geodesy, Seismology
Dr.-Ing. Omid Elmi	Remote Sensing
PD Dr.-Ing. habil. Johannes Engels	Physical Geodesy, Satellite Geodesy
Dr. Hassan Hashemi Farahani (until 30.6)	Physical Geodesy, Satellite Geodesy
M.Sc. Bruce Thomas (since 15.9)	Physical Geodesy, Satellite Geodesy
Dr.-Ing. Mohammad Tourian	Satellite Geodesy, Adjustment Theory
Ph.D. Rudolf Widmer-Schnidrig	Geophysics, Black Forest Observatory

Research Associates

M.Sc. Sajedeh Behnia	Satellite Altimetry
M.Sc. Dennis Mattes (until 30.11)	Satellite Altimetry
M.Sc. Saemian Peyman	Satellite Geodesy, Hydrology
M.Sc. Bo Wang	Satellite Altimetry

Administrative/Technical Staff

Dipl.-Ing. (FH) Thomas Götz	IT System, Controlling
Dipl.-Ing. (FH) Ron Schlesinger	IT System, Technical Support, Gravimetry
B.A. Tamara De Francesco (since 1.3)	Secretary

External Lecturers

Dipl.-Ing. Steffen Bolenz	Stadtmessungsamt, Stuttgart
Dipl.-Ing. Gerhard Grams	Ministerium für Ländlichen Raum und Verbraucherschutz Baden-Württemberg, Stuttgart
Dipl.-Ing. Dieter Heß	Ministerium für Ländlichen Raum und Verbraucherschutz Baden-Württemberg, Stuttgart

Guests

PhD student Bingshi Liu	University of Wuhan, Wuhan, China (1.9.2019–5.9.2020)
B.Sc. Clara Bützler	Universität Jena (since 1.10.2019)
Constance Chrismann	France (14.5.2020–30.9.2020)
Dr. Huanling Liu	CASM, Beijing, China (1.8.2019–31.1.2020)
Prof. Dr. Alfredo Ribeiro Neto	Universidade Federal de Pernambuco, Recife/PE, Brasilia (2.9.2019–31.7.2020)
Dr.-Ing. Shuang Yi	China (since 5.1.2019), Humboldt Fellow

Obituary of Prof. Erik Grafarend (1939–2020)

On 8 December 2020, Prof. Dr.-Ing.habil. Dr.tech.h.c.mult. Dr.-Ing.e.h.mult. Erik W. Grafarend, professor emeritus at the University of Stuttgart, died at the age of 81.

Erik Wilhelm Grafarend was born in Essen on 30 October 1939. After completing his studies in Mine Surveying (1964) at the University of Clausthal-Zellerfeld, Erik Grafarend pursued a rapid geodetic career with a doctorate (1966) and a second degree in physics (1968) at the same university. He moved to the University of Bonn where he habilitated in 1970 and received the Venia Legendi for the subject *Theoretical Geodesy*; the habilitation thesis was entitled *The Accuracy of a Point in Multidimensional Euclidean Space*. In 1971, at the young age of 32, he became an adjunct professor at the Institute for Theoretical Geodesy at the University of Bonn. This was followed in 1975 by an appointment to the chair of *Astronomical and Physical Geodesy* at the University of the Federal Armed Forces in Munich. In 1980, Prof. Grafarend was appointed successor to Prof. Karl Ramsayer at the University of Stuttgart, where he headed the Institute of Geodesy until 2005. Since his retirement in 2005, he continued to be active in geodesy as a researcher and, in particular, as a book author.

Prof. Grafarend's research activities were by no means limited to the actual dedication of his chair. Known for his extraordinarily broad interest, even curiosity, he covered a thematically wide spectrum of geodesy: physical geodesy, estimation theory, statistics, geodetic network design, satellite geodesy, differential geometry, map projections, geo-kinematics, earth rotation, inertial navigation, reference systems.

The diversity of his research is documented on the one hand in an extensive oeuvre of around 350 publications in relevant scientific journals and conference proceedings. On the other hand, Erik Grafarend has left a series of substantial books to geodetic posterity, amongst others *Map projections: cartographic information systems*, *Applications of linear and nonlinear models: fixed effects, random effects, and mixed models*. His most recent book projects include Gravitation and the editorship of the *Encyclopedia of Geodesy*. Beyond its diversity and size, Erik Grafarend's oeuvre is characterised by a creative power that has an almost artistic quality.

The geodetic work of Prof. Grafarend was highly recognised throughout his life. He was the first recipient of the prestigious Bomford Prize of the International Association of Geodesy in 1975. He has received numerous honorary doctorates and professorships from universities at home and abroad: Royal Institute of Technology in Stockholm (1989), TU Darmstadt (1996), TU Budapest (1998), University of the Federal Armed Forces in Munich (2000), University of Tehran (2002), University of Navarra in Pamplona (2014). He was a member of various learned societies: the German Geodetic Commission of the Bavarian Academy of Sciences, the Leibniz-Sozietät der Wissenschaften zu Berlin, the Finnish Academy of Sciences, the Hungarian Academy of Sciences, the Austrian Geodetic Commission.

In various functions in committees of national and international geodesy, Prof. Grafarend showed leadership. Within the DVW, he founded Working Group 7 *Experimental, Applied and Theoretical Geodesy*; for him, the name was the programme. As head of AK7, he founded the successful Geodetic Week, initially as an independent event with a special focus on young scientists, later established within InterGeo. In international geodesy, Erik Grafarend was clearly visible and, at conferences, also audible. In 1980 he was a founding editor of the journal *manuscripta geodaetica*, forerunner of the *Journal of Geodesy*. In the IAG he chaired various Special Study Groups and was elected President of the IAG Section IV *General Theory and Methodology* in 1983.

International networking has always been a special concern for Prof. Grafarend, but also a matter of course. He spent shorter and longer teaching and research stays in Columbus, Tehran, Wuhan, Sydney, Bandung, Uppsala, Stockholm and, regularly, Helsinki. Numerous top international scientists of the younger generation were motivated by him to conduct research with him in Stuttgart, among other things through funding from the Alexander von Humboldt Foundation. In recognition of his merits in promoting international scientific cooperation, he was awarded the Werner Heisenberg Medal of the Humboldt Foundation in 2000.

With Prof. Erik W. Grafarend we are losing a beacon of geodesy. He was an outstanding scientist whose interests and productivity knew hardly any boundaries, and whose contributions are inseparably linked to the development of modern geodesy. Nationally and internationally, he was valued as a colleague, as a teacher and, for many who knew him, as a friend. The beginnings of his scientific career could well have steered him into geophysics or physics. By a stroke of luck, geodesy became his home.

Research

Spatial downscaling of GRACE water storage change using a copula-supported Bayesian framework

The satellite missions GRACE and GRACE FO provided mass variations as a fundamentally new observation type for a wide spectrum of Earth science applications. They have fostered a number of novel applications in oceanography, geophysics, hydrology and hydrometeorology. Despite all the revolutionary findings, the utility of GRACE data has mainly been limited to large catchments due to their poor spatial resolution. We propose a method to downscale GRACE data by incorporating the data and the distribution of available high-resolution hydrological data and models. For this purpose, we propose a Bayesian framework that facilitates the estimation of downscaled GRACE data in the face of auxiliary data and their distribution. While it is common for Bayesian problems to consider a predefined model for the Bayesian ingredients (likelihood function and the prior distribution), we rely on the copula method to obtain nonparametric distributions from the data itself. We downscale the estimates of TWSC $\dot{S}_{\mathrm{G}}$ from GRACE with the help of two sources 1) hydrological measurements and 2) a hydrological model. For the hydrological measurements, we use precipitation minus evapotranspiration minus runoff $P - ET - R$ from ERA5, symbolized in the text as $\dot{S}_{\mathrm{H}}$. Our choice for the hydrological model is TWSC from the WGHM model $\dot{S}_{\mathrm{W}}$. The results show that the proposed methodology can successfully estimate downscaled GRACE terrestrial water storage changes and its uncertainty. As one example, Fig. 1, shows the results of downscaling for February 2003. Comparing the input fields from hydrological measurements $\dot{S}_{\mathrm{H}}$ (top row, left), WGHM model $\dot{S}_{\mathrm{W}}$ (top row, middle) and GRACE $\dot{S}_{\mathrm{G}}$ (top row, right), we observe a consistent TWSC ranging around -30 to -50 mm/month in the Upper Branco sub-basin. However, the three fields represent different TWSC in the river system of Amazon basin. While $\dot{S}_{\mathrm{W}}$ clearly distinguishes the river system, GRACE senses it as a smoothed field centered somewhere in the river and $\dot{S}_{\mathrm{H}}$ does not represent it at all. At each grid cell, $\hat{x}_{\mathrm{D}}$ (bottom row, left) represents the TWSC value with maximum posterior probability obtained within the developed Bayesian framework. In fact, $\hat{x}_{\mathrm{D}}$ represents the most plausible TWSC when considering data from hydrological measurements and the WGHM model as well as prior information from GRACE data. Its pattern shows that it is actually much more detailed in comparison to GRACE data, where the river system is recognized and some local patterns are captured including those over Andes Mountains. However, our downscaled TWSC in February 2003 over the floodplain of the Negro River seems to be dominated by the prior information (GRACE), leading to a positive TWSC in the presence of negative estimates by WGHM. Such a difference in inputs leads to a wider posterior distribution and thus to a larger uncertainty. The uncertainty map (second row, right) shows indeed a larger value of about 50 mm/month for the downscaled TWSC over the Negro River.

On large scales, say over the entire Amazon, GRACE should provide the best representation of total mass change over Amazon. Neither WGHM because of modelling uncertainty nor $P - ET - R$ because of uncertainty of individual measurements can deliver a realistic rep-

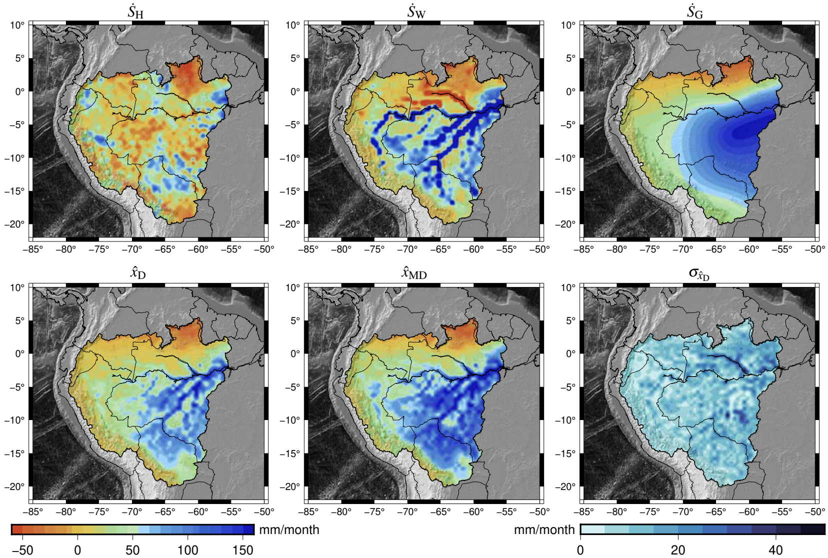

Figure 1: Terrestrial water storage change from hydrological measurements $\dot{S}_{\mathrm{H}}$ (top left), WGHM model $\dot{S}_{\mathrm{W}}$ (top middle) and GRACE $\dot{S}_{\mathrm{G}}$ (top right) together with the downscaled results: MAP estimate $\hat{x}_{\mathrm{D}}$ (bottom left), mass-conserved MAP estimate $\hat{x}_{\mathrm{MD}}$ (bottom middle) and uncertainty of downscaled results $\sigma_{\hat{x}_{\mathrm{D}}}$ (bottom right) for February 2003

resentation of total mass change over the entire Amazon. As a result, $\hat{x}_{\mathrm{D}}$ is not expected to preserve the mass conservation property. This is because the Bayesian framework is set for each grid cell and each month individually and not designed to be constrained by a condition for the whole basin. In order to fulfill the mass conservation over the entire Amazon, a mass-conserved solution is estimated by assuming that the cumulative distribution of downscaled TWSC $\hat{x}_{\mathrm{D}}$ should obey cumulative distribution of GRACE over the entire Amazon. Therefore, through applying a classical CDF matching we obtain a mass-conserved MAP estimate, for which the spatial distribution pattern of the TWSC remains intact and only the distribution of the data in terms of their quantiles would change. The mass-conserved MAP estimate $\hat{x}_{\mathrm{MD}}$ provides an even more detailed TWSC in comparison to $\hat{x}_{\mathrm{D}}$. For instance, large TWSC values in the Ucayali River, seen in the WGHM data, are also partially captured in $\hat{x}_{\mathrm{MD}}$.

The results show that the proposed methodology can successfully downscale the TWSC and help us to understand the variation in water storage changes in many small catchments[1]. It should be noted that the performance of the results depends on the quality of the input data. However, even if the input data comes with high inconsistencies, the main advantage

[1] Mohammad J. Tourian and Nico Sneeuw, Spatial downscaling of GRACE water storage change using a copula-supported Bayesian framework, Journal of Geodesy (under review)

of the proposed copula-supported Bayesian framework is that it takes the uncertainties associated with the data and models into account and provides an uncertainty together with the estimation.

Developing an outlier identification scheme for inland altimetric water level time series

That satellite altimetry has proven effective in monitoring inland water bodies is beyond doubt. Over the last few decades, the scientific community has developed significant knowledge and experience in using altimetry data for monitoring lakes, reservoirs and rivers. With the Copernicus Sentinel-3A and Sentinel-3B in orbit, satellite altimetry has already entered an operational stage; the implication being that we need clear measures of its success. This becomes even more noticeable when taking into account the recently launched Sentinel-6 Michael Freilich and the Surface Water and Ocean Topography (SWOT) mission, foreseen to be launched in late 2022.

Despite all technical and methodological developments, scientific and water management communities are far from exploiting the full potential offered by the three-decade-long altimetry measurements. This becomes evident when comparing the number of altimetry tracks crossing continental water bodies with the number of virtual stations permanently monitored by the available databases, e.g. HydroSat, Hydroweb, DAHITI, etc. To attain and maintain a global network of virtual gauging stations, however, is an indispensable need. This is to help scientists in keeping track of the fresh water resources and water authorities in decision making.

Altimetric water level time series over inland waters are substantially affected by outliers. This is mainly rooted in disproportionality between the crossover width and radar footprint size, leading to heterogeneous radar reflections, off-nadir measurements, and less characterized waveforms. The problem is unavoidable even when using the most sophisticated retracking algorithms and processing schemes. In our research, we focus on removing (or identifying) these outliers at the level of time series analysis. Removing outliers in time series of inland altimetry is however hindered by a number of factors: irregular sampling, low signal-to-noise-ratio, long periods of no data, short-duration time series, and interruptions in the natural flow of the target water body. To deal with these challenges, we propose an automated, data-driven outlier rejection methodology designed within an iterative, non-parametric adjustment scheme. The algorithm comprises using Singular Spectrum Analysis (SSA) for gap-filling, Savitzky-Golay filtering for smoothing, and a specially developed outlier identification method. The identification method is novel in that it entails a local definition of an 'outlier' and hence, a unique statistical distribution.

The algorithm is applied to water level time series of various case studies derived from different altimetry missions. At a confidence level of 99 %, our validation shows an average success rate of 80 % in identifying the already flagged outliers. Figure 2 illustrates the outcome of the proposed algorithm for a virtual station of Jason-2 altimetry mission over the

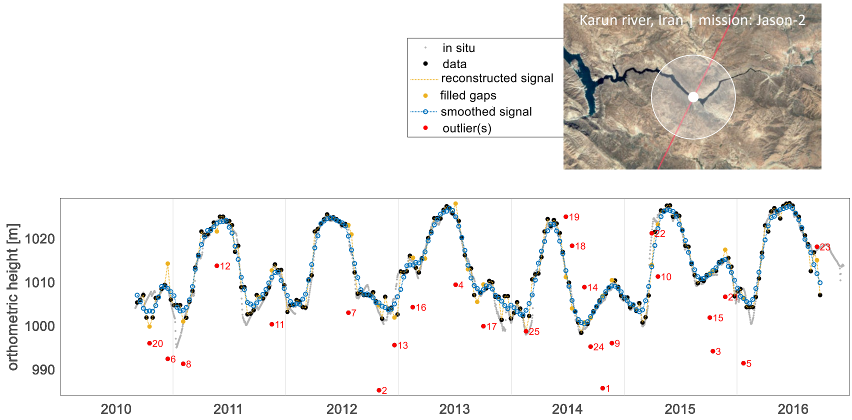

Figure 2: The result of outlier rejection algorithm applied to a time series of Jason-2 altimetry mission over a mountainous, narrow river crossing in Karun, Iran.

river Karun in Iran. The crossing width is about 320 m with the altimetry track located in a highly mountainous region.

Estimating Water Level, Area and Volume Changes of Lakes during 1984–2020 Using ICESat-2 Altimetry and Landsat Imagery

To monitor water volume change, the conventional and very precise method is to build gauge stations, but it's costly to build and maintain, and it's also difficult for remote regions. Nowadays the method widely used is combing radar altimetry data and images, but it's still not easy to get the simultaneous data of water level and area, and a problem is that altimetry data are not available before 1992. The other methods such as shipborne sonar or echo sounder or airborne bathymetry lidar are very costly and inefficient, especially for politically sensitive regions. We consider to use ICESat-2 satellite with high spatial resolution, which provides a new opportunity to monitor water level-area-volume change with satellite images.

The scenario is to estimate the water area from the image classification, and to estimate the water level from the intersections between water boundaries and ICESat-2 tracks.

For water-land classification, firstly, we generated clipped Landsat images with annually averaged reflection of images in each year by the Google Earth Engine (GEE) platform. Secondly, the Modification of the Normalized Difference Water Index (MNDWI) was applied for creating a binary classification (water and land). A threshold of MNDWI between 0.12 to 0.17 was selected for lakes.

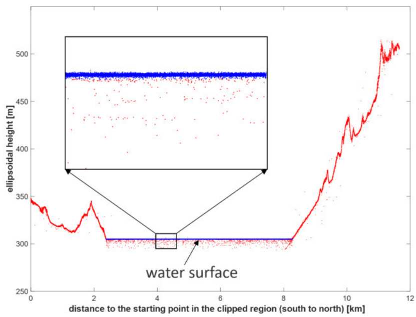

(a) *Extracted point cloud of water surface (blue points)*

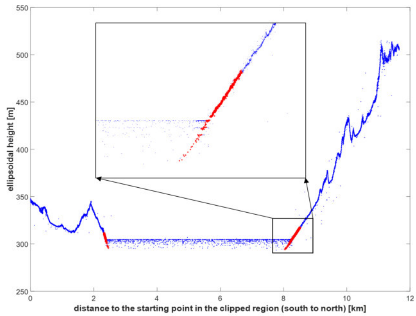

(b) *Near shore topography points (red points) extracted after applying RANSAC*

Figure 3: Schematic of laser data processing

For ICESat-2 laser data processing, our aim is to get a clean point cloud topography profile of the tracks. Firstly, we employed the algorithm called Density Based Spatial Clustering of Applications with Noise (DBSCAN) to eliminate noise and to extract a relatively clean point cloud (Fig. 3(a)). After removing the water surface, there are still many noisy points under the water surface, which are from reflections of water volume. We assume the near shore region (the topography above and under the water surface) has a linear slope. In that case it is suitable to use the RANSAC algorithm to extract the points in the near shore region. From Fig. 3(b), we can see the limit of bathymetry was enlarged, but the points under the water surface should be corrected by Snell's law because of refraction.

To estimate the water level, the processed laser tracks were projected on the classified water-land images. In Fig. 4 we use two tracks, which will have 4 intersections. The points within a 30 m radius of the intersections were selected. Then we use RANSAC to get the best fitting straight line, and interpolate the heights of intersections. Therefore, the water level is the mean value of the heights of 4 intersections.

Fig. 5(a) shows our method gives an RMSE of 1.01 m between the estimated water level result and in-situ data, and we can see with the lake floor topography measurement, the water level can also be estimated even the water surface is above the bathymetry limit. As the water area and the water level of each year estimated, the level-area model is established, which represents a near-linear relation (Fig. 5(b)).

Since the water level and area were estimated for each year, the water volume variation can be calculated by geometric models. Comparing with in-situ data, our method shows an RMSE of 0.4395 km^3, relative to a volume variation of about 20 km^3.

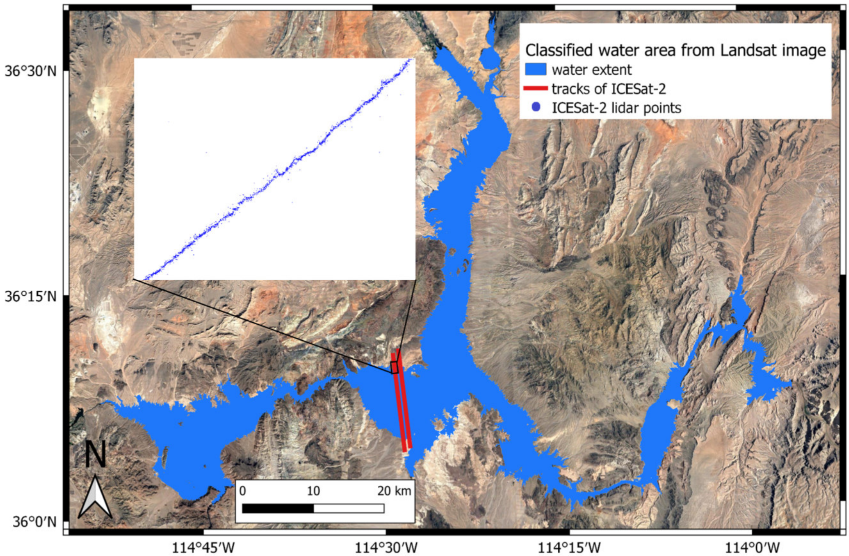

Figure 4: Extracted Water mask and laser track projected on the map of Lake Mead

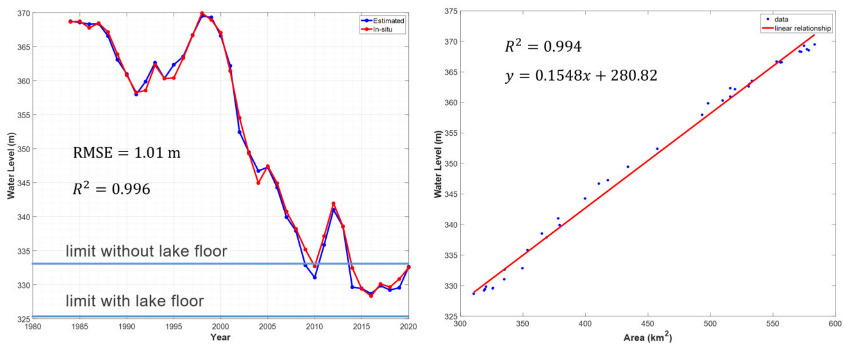

(a) *Water level comparison between our method and in-situ data (1984-2020)*

(b) *Relationship of estimated water level and area*

Figure 5: Comparisons of water level and area

Data-driven and physically informed modelling of the terrestrial water storage dynamics

The successful GRACE mission and now its successor GRACE Follow-On, has provided Earth scientists with unprecedented insights into how mass is redistributed across the Earth's surface and subsurface. In particular, hydrologists are now able to map globally and on a monthly basis the variations of terrestrial water storage, which is a fundamental component of the water cycle. The analysis of the spatio-temporal variability of this field has enabled scientists to quantify the impact of natural climatic variability on the water cycle but has also revealed the anthropogenic origin of some observed trends in groundwater depletion.

Going one step forward, we attempt in this work to infer from data a dynamical model of the water flow at sub-basin scales and thereby, a model of the natural fluctuations of the terrestrial water storage. Such a model will for instance facilitate the forecast of storm flows or help better quantify the response of a catchment to a period of low or no precipitation. We follow a data-driven approach constrained by first principles and borrow tools and concepts developed in the fields of dynamical system and control theory.

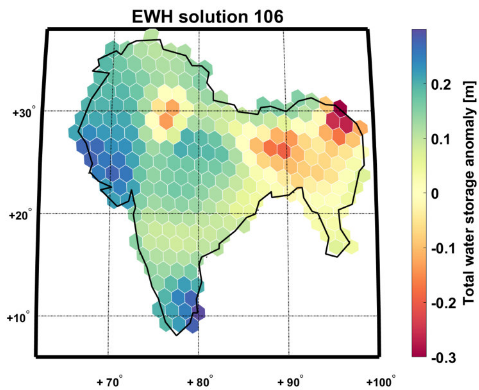

Figure 6: Example of the division of the Indian subcontinent into arbitrary sub-regions.

A given region of interest is first divided into arbitrary sub-regions of equal areas (see Fig. 6) and for which we compute the time series of monthly terrestrial water storage anomaly and the input of precipitation water corrected for the evapotranspiration. To begin, we only consider linear models where the drainage of each sub-region is supposed to be proportional to its total water storage. The main objective is then to infer from the data the large matrix encoding the network of water flux between the different sub-regions. The use of dynamical mode decomposition (DMD) seems to be a promising algorithm to determine this matrix while tackling the potential problem of high dimension.

Gravimeter search for compact dark matter objects (CDOs) moving inside Earth

Figure 7: View of the superconducting gravimeter SG-056 in the BFO mine, 150m below the surface. A walk-in refrigerator chamber houses the instrument and protects it from the harsh environment in the mine. The blue dewar can be seen with the shiny cold head on top. The gravity sensor is located inside the dewar above a liquid Helium bath. The coldhead cools the inside of the dewar to 4 Kelvin.

Many experiments to directly detect dark matter have not yet seen a clear signal. Dark matter, or one component of it, could be composed of compact dark objects (CDOs). These objects are assumed to have small non-gravitational interactions with normal matter. Microlensing observations rule out most of dark matter being made of CDOs with masses between $10^{-11} M_\odot$ and $15 M_\odot$. Here $M_\odot$ is the solar mass. In this paper, we focus on CDOs with masses between about 10^{-19} and $10^{-11} M_\odot$. We assume the objects are not black holes (to avoid destroying the Earth) but otherwise try to minimize our assumptions about detailed CDO properties.

An object moving in a circular orbit, through an average density $\bar{\rho}$, will orbit with period T and frequency ν given by Kepler's 3rd law,

$$\nu = \frac{1}{T} = \left(\frac{1}{3\pi} G \bar{\rho}\right)^{1/2} . \tag{1}$$

The density of the Earth $\rho(r)$ as specified in the PREM model (Dziewonski and Anderson, 1981) is plotted in Fig. 8 along with the average density $\bar{\rho}(r)$ of matter interior to radius r. The orbital frequency ν varies from ≈ 0.3 mHz for small r to 0.2 mHz at the surface. Near the center of the Earth $\bar{\rho} \approx \rho_c = 13.1$ g/cm^3 and is nearly constant. For a constant density, the

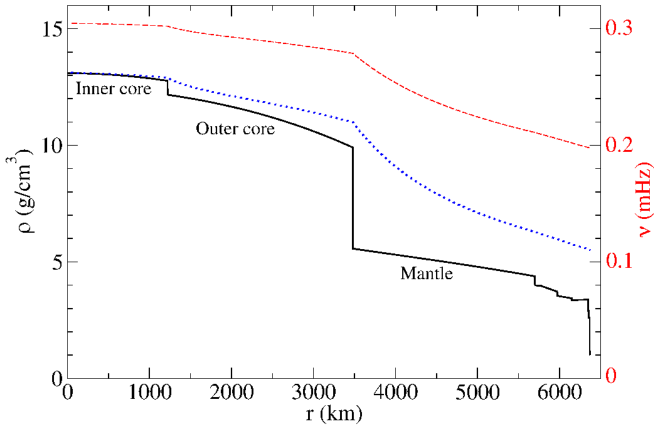

Figure 8: Density $\rho(r)$ of the PREM Earth model versus radius r (solid black line). The dotted blue line shows the average density (of matter interior to r) $\bar{\rho}(r)$. Finally the orbital frequency ν for a circular orbit inside the Earth of radius r is shown as the dashed red line using the righthand scale.

orbits are ellipses with the center of the ellipse coincident with the center of the Earth and the period is independent of r.

Gravimeters on the surface of the Earth could be sensitive to CDOs moving in the inner core by looking for very small periodic changes in the local acceleration from gravity (little g) with period near $T = 55$ min or frequencies near $\nu(\bar{\rho} = \rho_c) = \nu_0 = 0.305$ mHz (or somewhat smaller for larger radius orbits). In general, we don't know m_D or the radius of the orbit. However, we know the (approximate) orbital frequency ν_0 because we know the density profile inside the Earth.

We now analyze gravimeter data. A number of superconducting gravimeters (SGs) have been deployed at various locations around the world. The sensor self-noise of these instruments improved in 2009 when the manufacturer increased the mass of the levitated proof mass from 4 to 17.2 g. At the Black Forest Observatory (BFO) in South-Western Germany the first of these new SGs was installed and because of its low noise level we will concentrate our analysis on data from that instrument.

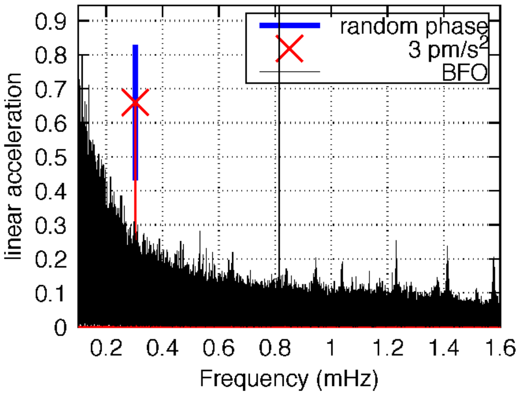

Figure 9: Fourier amplitude spectrum of gravity residuals at the Black Forest Observatory. The time series starts on July 20, 2011 and is 6.7 years long. The gravity data have been corrected for the atmospheric pressure with an admittance of -3.0 nm s^{-2}/hPa. The red line with a cross shows calibration injections at a frequency of 0.303 mHz with an amplitude of 3 pm/s^2 and different initial phases shown by the blue band.

In Fig. 9 we show the Fourier amplitude spectrum of the pressure corrected and Hanning tapered gravity residuals from BFO. A number of background signals are visible. A narrow, large amplitude spectral peak is seen near 0.8 mHz. This is the fundamental monopole ($\ell = 0$) free oscillation ${}_0S_0$ (or breathing mode) of the Earth. This mode has a high Q factor ($Q = 5500$) and can remain excited for several months after a large earthquake. Next to ${}_0S_0$ fundamental spheroidal free oscillation modes of the Earth (${}_0S_\ell$) with angular order from $\ell = 3$ to 9 are seen near 0.46, 0.64, 0.84, 1.03, 1.23, 1.41, and 1.57 mHz. These modes are excited by large quakes.

In Fig. 9 we have also included a harmonic signal at 0.3 mHz (red) with a 3 pm/s^2 time-domain amplitude which is clearly above the background noise level. This 3 pm/s^2 amplitude can be translated into an upper bound for the mass of a CDO moving inside Earth: we rule out CDOs moving in the Earth unless their masses m_D and or orbital radii a are very small so that $m_D\, a < 1.2 \times 10^{-13} M_\oplus R_\oplus$. Here $M_\oplus$ and $R_\oplus$ are the mass and radius of the Earth. For $a \geq 0.1\, R_\oplus$, this rules out orbiting CDOs with masses above 7×10^{12} kg. This bound on the CDO mass is over a million times smaller than the $10^{-11} M_\odot$ lowest mass probed by microlensing.

One can search for CDOs in other solar system bodies and we are currently analyzing the data from the NASA InSight mission for signs of CDOs moving inside Mars.

Spaceborne river discharge from a nonparametric stochastic quantile mapping function

The number of active gauges with open-data policy for discharge monitoring along rivers has decreased over the last decades. Therefore, spaceborne measurements are investigated as alternatives. Among different techniques for estimating river discharge from space, developing a rating curve between the ground-based discharge and spaceborne river water level or width is the most straightforward one. However, this does not always lead to successful results, since the river section morphology often cannot simply be modeled by a limited number of parameters. Moreover, such methods do not deliver a proper estimation of the discharge's uncertainty as a result of the mismodeling and also the coarse assumptions made for the uncertainty of inputs.

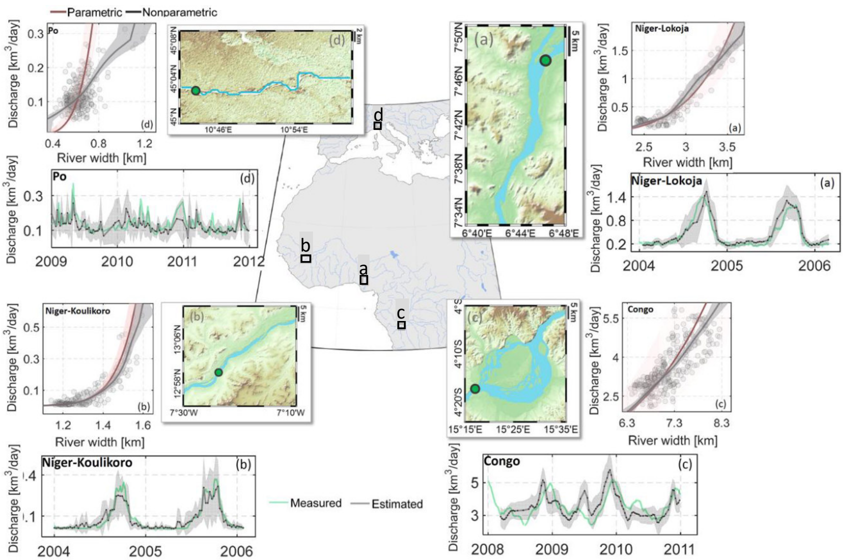

Figure 10: Four river reaches defined as case studies. Reaches (a) and (b) are river reaches over the Niger River, (c) is part of Congo River and (d) is selected over the Po River. For each case, the developed rating curve model and stochastic mapping function are plotted on top of the scatterplot of the simultaneous width and discharge measurements. Moreover, time series of estimated discharge using the proposed algorithm (black dots) is compared to the in situ discharge duirng the validation period.

We propose an algorithm for developing a nonparametric model for estimating river discharge and its uncertainty using spaceborne river width measurements. The algorithm employs a stochastic quantile mapping function scheme by, iteratively: 1) generating realizations of river discharge and width time series using Monte Carlo simulation, 2) obtaining a collection of quantile mapping functions by matching all possible permutations of simulated river discharge and width quantile functions, 3) adjusting the measurement uncertainties according to the point cloud scatter. The algorithm performs the same steps in the next iterations after updating the input measurement uncertainties until the convergence condition is satisfied.

The proposed method is applied over four river reaches with different dynamic behaviour along Niger, Congo and Po rivers. Evaluating the estimates shows that the performance of the proposed method is superior to the conventional rating curve technique especially in challenging cases. Over the Niger river reaches, the improvement is moderate and the performance of both techniques is similarly in acceptable range. The RMSEs were less than 10 % and the NSE coefficients were about 0.9. In the Congo river reach the NSE improved from 0.17 to 0.31, because the stochastic quantile mapping function can mitigate the effect of noisy measurements. Over the Po river reach, through coping with the mismodelling error, the proposed method improved the NSE coefficient from −9 to 0.13 and reduced RMSE from 52 % to 15 %.

Table 1: Statistical indices for the performance assessment. The results for each technique are presented in two lines: (1) rating curve technique, (2) stochastic quantile mapping function

River	**Corr.** [ ]	**RMSE** [%]	**NSE** [ ]
Niger-Lokoja	0.95 0.96	9.3 8.9	0.89 0.90
Niger-Koulikoro	0.96 0.96	8.8 9.1	0.90 0.90
Congo	0.64 0.64	23.0 20.5	0.17 0.31
Po	0.46 0.46	52.1 15.3	−8.90 0.13

Releasing from the bottleneck of characterizing the river section geometry through a limited number of model parameters is, in fact, the main reason for the obtained better performance. However, the performance of the technique highly depends on the availability of enough measurements in both datasets. It means that if a certain percentile is not represented in the quantile functions of both variables, the model will rely on interpolation for estimating discharge on that percentile.

How much water did Iran lose over the last two decades?

Iran, located in the south-west of Asia, is currently facing water scarcity. Aggressive exhaustion of non-renewable water to satisfy the country's growing demand, has led to a suite of environmental and socio-economic problems across the country. With the lack of conclusive measurement of total water storage, our knowledge of Iran's water loss is still incomplete. Gravity Recovery and Climate Experiment (GRACE) mission and its successor, GRACE Follow-On (GRACE-FO), caused a quantum leap in the hydrological understanding. Despite its course spatial resolution, satellite gravimetry observes the change in water stored in deep soil and aquifers below Earth's surface which is very sparsely measured worldwide. Our results from the analysis of satellite gravimetric data (GRACE and GRACE Follow-On) indicate that Iran has lost 211 ± 34 km^3 of its total water storage during the last 17 years corresponding to an alarming rate of -12 ± 2 km^3/yr (Fig. 11). Such a tremendous water loss happened despite an increased precipitation rate of $+4.9 \pm 0.02$ km^3/yr (Fig. 12).The discrepancies between total water storage loss and precipitation gain can only be explained with the drastic drop (-28 ± 1.4 cm/yr) in the mean groundwater level caused by overexploitation of non-renewable water resources.

The 2007 drought triggered the increasing demand of farmers to use groundwater in the lack of surface water resources. As a result, total water storage ended up in to a new equilibrium by the end of 2016. Extreme precipitation leading to flood events in early 2019 compensated for the water loss in the previous years, but could not recover the groundwater storage. Our results shows that Iran's water storage will go back to the state of 2003 in 12 years (2031) with the absence of extreme droughts, continuation of the recent rainfall pattern, and assuming no acceleration in the anthropogenic activities like groundwater withdraw.

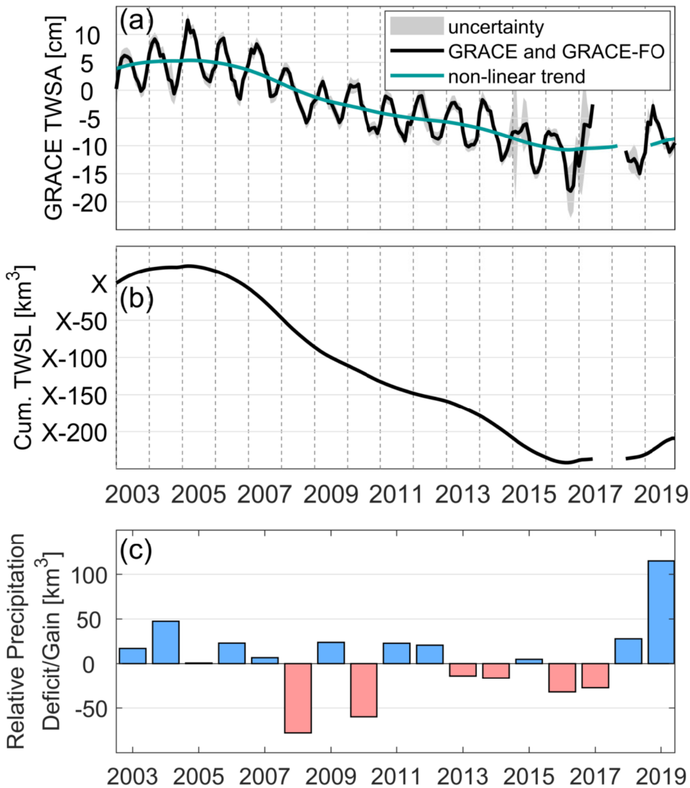

Figure 11: (a) TWSA derived from GRACE and GRACE-FO over Iran. The error envelope represents the uncertainty of the processed data. The non-linear trend is achieved using SSA algorithm with 24 month window. (b) Time evolution of the accumulated total water storage loss over the last 17 years, considering the total water storage of Iran as X in 2003. (c) Inter-annual variation of the relative losing water status (red) or gaining water status (blue) from precipitation over Iran with respect to the long-term mean (1983–2002).

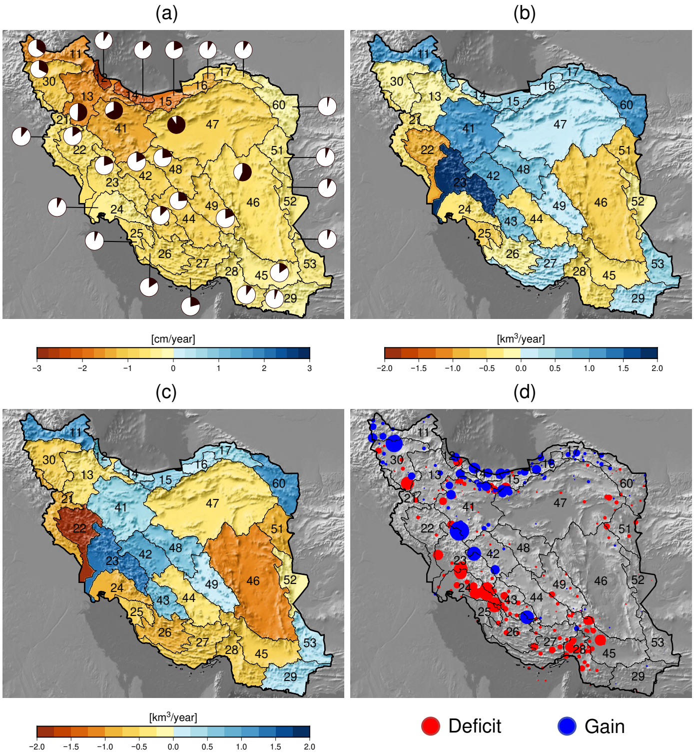

Figure 12: (a) Basin-wise distribution of TWS loss rate from 2003 to 2019. The volumetric TWS loss rates are shown in km^3 per year using circular gauges, while the whole circle represent $2\,km^3$/year annual losing rate. (b) Relative deficit or gain in precipitation calculated from the selected precipitation datasets for the period 2003–2019. (c) same as (b) but for the period 2003–2016. (d) Relative deficit or gain in precipitation calculated from in-situ gauges for the period 2003–2019. The radius of the bubbles at each station represents the magnitude of gain or deficit.

Publications

(`https://www.gis.uni-stuttgart.de/en/research/publications/index.html`)

Refereed Journal Publications

Anderson, A. N., J. H. Foster, and N. Frazer (2020): Implications of deflation-inflation event models on Kīlauea Volcano, Hawaii. In: *Journal of Volcanology and Geothermal Research* 397. issn: 0377-0273. doi: `10.1016/j.jvolgeores.2020.106832`.

Banfield, D., A. Spiga, SEISteam, and R. Widmer-Schnidrig (2020): The atmosphere of Mars as observed by InSight. In: *Nature Geoscience* 13, pp. 190–198. doi: `10.1038/s41561-020-0534-0`.

Cambiotti, G., K. Douch, S. Cesare, R. Haagmans, N. Sneeuw, A. Anselmi, A. M. Marotta, and R. Sabadini (2020): On Earthquake Detectability by the Next-Generation Gravity Mission. In: *Surveys in Geophysics* 41.5, pp. 1049–1074. doi: `10.1007/s10712-020-09603-7`.

Ferreira, V. G., B. Yong, M. Tourian, C. E. Ndehedehe, Z. Shen, K. Seitz, and R. Dannouf (2020): Characterization of the hydro-geological regime of Yangtze River basin using remotely-sensed and modeled products. In: *Science of The Total Environment* 718. issn: 0048-9697. doi: `10.1016/j.scitotenv.2020.137354`.

Foster, J. H., T. L. Ericksen, and B. Bingham (2020): Wave Glider–Enhanced Vertical Seafloor Geodesy. In: *Journal of Atmospheric and Oceanic Technology* 37.3, pp. 417–427. doi: `10.1175/jtech-d-19-0095.1`.

Garcia, R. F., B. Kenda, T. Kawamura, A. Spiga, N. Murdoch, P. H. Lognonné, R. Widmer-Schnidrig, N. Compaire, G. Orhand-Mainsant, D. Banfield, and W. B. Banerdt (2020): Pressure Effects on the SEIS-InSight Instrument, Improvement of Seismic Records, and Characterization of Long Period Atmospheric Waves From Ground Displacements. In: *Journal of Geophysical Research: Planets* 125.7. doi: `10.1029/2019JE006278`.

Ghobadi-Far, K., S.-C. Han, S. Allgeyer, P. Tregoning, J. Sauber, S. Behzadpour, T. Mayer-Gürr, N. Sneeuw, and E. Okal (2020): GRACE gravitational measurements of tsunamis after the 2004, 2010, and 2011 great earthquakes. In: *Journal of Geodesy* 94.65, pp. 1–9. doi: `10.1007/s00190-020-01395-3`.

Horowitz, C. J. and R. Widmer-Schnidrig (2020): Gravimeter Search for Compact Dark Matter Objects Moving in the Earth. In: *Phys. Rev. Lett.* 124.5. doi: `10.1103/PhysRevLett.124.051102`.

Kenda, B., M. Drilleau, R. F. Garcia, T. Kawamura, N. Murdoch, N. Compaire, P. Lognonné, A. Spiga, R. Widmer-Schnidrig, P. Delage, V. Ansan, C. Vrettos, S. Rodriguez, W. B. Banerdt, D. Banfield, D. Antonangeli, U. Christensen, D. Mimoun, A. Mocquet, and T. Spohn (2020): Subsurface Structure at the InSight Landing Site From Compliance Measurements by Seismic and Meteorological Experiments. In: *Journal of Geophysical Research: Planets* 125.6. doi: `10.1029/2020JE006387`.

Lin, Y., X. Li, T. Zhang, N. Chao, J. Yu, J. Cai, and N. Sneeuw (2020): Water Volume Variations Estimation and Analysis Using Multisource Satellilte Data: A Case Study of Lake Victoria. In: *Remote Sensing* 12.18, pp. 1–22. doi: `10.3390/rs12183052`.

Lognonné, P., W. Banerdt, SEISteam, and R. Widmer-Schnidrig (2020): Constraints on the shallow elastic and anelastic structure of Mars from InSight seismic data. In: *Nature Geoscience* 13, pp. 213–220. doi: `10.1038/s41561-020-0536-y`.

Saemian, P., O. Elmi, B. Vishwakarma, M. Tourian, and N. Sneeuw (2020): Analyzing the Lake Urmia restoration progress using ground-based and spaceborne observations. In: *Science of The Total Environment*. doi: `10.1016/j.scitotenv.2020.139857`.

Scholz, J.-R., R. Widmer-Schnidrig, P. Davis, P. Lognonné, B. Pinot, R. F. Garcia, K. Hurst, L. Pou, F. Nimmo, S. Barkaoui, S. de Raucourt, B. Knapmeyer-Endrun, M. Knapmeyer, G. Orhand-Mainsant, N. Compaire, A. Cuvier, É. Beucler, M. Bonnin, R. Joshi, G. Sainton, E. Stutzmann, M. Schimmel, A. Horleston, M. Böse, S. Ceylan, J. Clinton, M. van Driel, T. Kawamura, A. Khan, S. C. Stähler, D. Giardini, C. Charalambous, A. E. Stott, W. T. Pike, U. R. Christensen, and W. B. Banerdt (2020): Detection, Analysis, and Removal of Glitches From InSight's Seismic Data From Mars. In: *Earth and Space Science* 7.11. doi: `10.1029/2020ea001317`.

Stähler, S. C., R. Widmer-Schnidrig, J.-R. Scholz, M. van Driel, A. Mittelholz, K. Hurst, C. L. Johnson, M. T. Lemmon, R. D. Lorenz, P. Lognonné, N. T. Müller, L. Pou, A. Spiga, D. Banfield, S. Ceylan, C. Charalambous, J. Clinton, D. Giardini, F. Nimmo, M. Panning, W. Zürn, and W. B. Banerdt (2020): Geophysical observations of Phobos transits by InSight. In: *Geophysical Research Letters* 47.19. doi: `10.1029/2020GL089099`.

Yi, S., C. Song, K. Heki, S. Kang, Q. Wang, and L. Chang (2020b): Satellite-observed monthly glacier and snow mass changes in southeast Tibet: implication for substantial meltwater contribution to the Brahmaputra. In: *The Cryosphere* 14.7, pp. 2267–2281. doi: `doi.org/10.5194/tc-14-2267-2020`.

Zhang, J., M. Tourian, and N. Sneeuw (2020): Identification of ENSO signature in the boreal hydrological cycle through canonical correlation with sea surface temperature anomalies. In: *International Journal of Climatology*, pp. 1–23. doi: `10.1002/joc.6573`.

Books & Miscellaneous

Cai, J., D. Dong, N. Sneeuw, and Y. Yao (2020): "Converted Total Least Squares Method and Gauss-Helmert Model with Applications to Coordinate Transformations". In: *IX Hotine-Marussi Symposium on Mathematical Geodesy*. Ed. by P. Novák, M. Crespi, N. Sneeuw, and F. Sansò. Cham: Springer International Publishing, pp. 117–125. isbn: 978-3-030-54267-2.

Conference Presentations

Behnia, S., M. J. Tourian, and N. Sneeuw (2020): *How to Get Rid of Outliers in Time Series of Inland Altimetry?* (Earth Observation for Water Cycle Science 2020, ESA, online, 16–19 November).

Bo Wang, Mohammad Tourian, N. S. (2020): *Coastal Altimetry using ICESat-2 Photon-Counting Laser Altimeter*. (ESA 12th Coastal altimetry workshop, Frascati, Italy).

Camici, S., L. Brocca, C. Massari, G. Giuliani, N. Sneeuw, H. Hashemi Farahani, M. Restano, and J. Benveniste (2020): *An observation-based approach for global runoff estimation: exploiting satellite soil moisture and GRACE*. (EGU 2020, Vienna, 4–8 May). url: `https://doi.org/10.5194/egusphere-egu2020-13718`.

Douch, K., C. Bützler, G. Cambiotti, S. Cesare, N. Sneeuw, A. Anselmi, A. M. Marotta, and R. Sabadini (2020): *Observation of earthquake co- and post-seismic signals with the Next Generation Gravity Mission (NGGM)*. (The present and future of satellite gravimetry, Workshop, Kanpur, India).

Douch, K., P. Saemian, and N. Sneeuw (2020): *Investigating Granger causality with state-space representation of time series: a case study of the total water storage anomaly over Australia*. (EGU General Assembly Conference Abstracts).

Mattes, D., M. Losch, B. Rabe, M. Tourian, and N. Sneeuw (2020): *Response of Arctic sea level and hydrography to hydrological regime change over boreal catchments (RASLyBoCa)*. talk. SPP annual meeting, Bonn, Germany. url: `https://www.gis.uni-stuttgart.de/forschung/doc/Mattes_2020a.pdf`.

Saemian, P., M. Tourian, and N. Sneeuw (2020a): *Storage-based Drought Indices Using Satellite Gravimetry and External Climatology*. (AGU Fall Meeting 2020).

Saemian, P., M. Tourian, and N. Sneeuw (2020b): *The uncertainty of storage-based drought indices from GRACE*. (EGU General Assembly Conference Abstracts).

SaWaMteam and S. Behnia (2020): *Seasonal Water Management for Semi-Arid Areas*. (GRoW final conference).

Tourian, M. J., O. Elmi, S. Behnia, and N. Sneeuw (2020): *Defining a retracking manifold within a radargram stack to improve satellite altimetric water level over coastal seas: A feasibility study*. (ESA 12th Coastal altimetry workshop, Frascati, Italy).

Tourian, M. J. and N. Sneeuw (2020): *Spatial downscaling of GRACE water storage change using a Bayesian approach supported by copula*. (The present and future of satellite gravimetry, Workshop, Kanpur, India).

Yi, S. and N. Sneeuw (2020): *Emerging instability in global terrestrial water storage since 2010*. (EGU 2020, Vienna, 4–8 May). url: `https://doi.org/10.5194/egusphere-egu2020-17922`.

Yi, S., N. Sneeuw, J. Foster, and Y. Pan (2020a): *Intense drought in the Island of Hawaii and its modulation on magma upwelling*. (The present and future of satellite gravimetry, Workshop, Kanpur, India).

Master Theses

(`https://www.gis.uni-stuttgart.de/lehre/abschlussarbeiten/`)

Bützler, Clara: Gravity gradients of prompt elasto-gravity signals. Aspects of their simulation and the posibility to mesure them - A case study for the Tohoku Oki earthquake.

Chen, Yiming: Investigation of the relationship between satellite altimetry and the environment by multisensor spaceborne data

Daud Gisiri, Thomas: Analyzing the long term variations of ocean mass in Arctic region using satellite gravimetry

Liu, Mo: Better understanding of permafrost in Lena and Yenisei river basins

Naangmenkuu, Casimir: Assessing the potential of using GNSS-R technology in GhanaSat-2: a simulation study

Eitel, Maximilian: Application of Image Segmentation Techniques in Satellite Altimetry Retracking: a Feasibility Study

Bachelor Theses

(`https://www.gis.uni-stuttgart.de/lehre/abschlussarbeiten/`)

Gou, Junyang: Estimation of significant wave height using Sentinel-3 data

Knogl, Robin: Vorverarbeitung von Satellitenaltimetriedaten für die Analyse des zeitlich-variablen Schwerefelds

Schneider, Nicholas: Analyzing the spatio-temporal behavior of Poyang Lake using Google Earth Engine

Ziqing, Yu: Understanding the positive trend in total water storage of OB river using spaceborn observation

Internship Report

Chrisman, Constance: Analysis of satellite altimetry bias over lakes

Guest Lectures and Lectures on special occasions

Activities in National and International Organizations

Sneeuw N.

Professor h.c. (Luojia chair), Wuhan University, China
Adjunct Professor of the College of Engineering, University of Tehran
Fellow International Association of Geodesy (IAG)
Full Member Deutsche Geodätische Kommission (DGK)
Chair, Assessment Panel Space Research, NWO, Netherlands
Member of Gauss-Gesellschaft e.V.
Member of the editorial board of Surveys in Geophysics
Member of the editorial board of Studia Geophysica et Geodaetica

Tourian M.

Member of SWOT Science Team

Widmer-Schnidrig R.

Member of Mars-InSight Science Team (NASA)

Courses – Lecture/Lab/Seminar

Bachelor Geodesy & Geoinformatics (German):

Amtliches Vermessungswesen und Liegenschaftskataster (Grams)	2/0/0/0
Einführung Geodäsie und Geoinformatik (Sneeuw)	2/2/0/0
Integriertes Praktikum/Integrated Field Work (Sneeuw)	10 days
Landesvermessung (Foster, Mattes)	2/2/0/0
Physikalische Geodäsie (Sneeuw)	2/2/0/0
Referenzsysteme (Sneeuw, Antoni)	2/2/0/0
Satellitengeodäsie (Sneeuw, Douch)	1/1/0/0
Wertermittlung (Bolenz)	2/0/0/0

Master Geodesy & Geoinformatics (German):

Aktuelle Geodätische Satellitenmissionen (Sneeuw)	2/2/0/0
Amtliche Geoinformation (Heß)	2/0/0/0
Ausgewählte Kapitel der Parameterschätzung (Tourian)	2/2/0/0
Geodynamische Modelle (Engels)	2/2/0/0
Koordinaten- und Zeitsysteme in der Geodäsie (Tourian)	2/0/0/0
Physikalische Geodäsie (Engels, Sneeuw, Antoni)	2/2/0/0
Satellitengeodäsie (Sneeuw, Antoni)	2/1/0/0

Master GeoEngine (English):

Advanced Mathematics (Foster, Thomas)	3/2/0/0
Foundations of Satellite Geodesy (Sneeuw, Douch)	2/1/0/0
Integriertes Praktikum/Integrated Field Work (Sneeuw)	10 days
Map Projections and Geodetic Coordinate Systems (Foster, Thomas)	2/1/0/0
Physical Geodesy (Sneeuw, Hashemi Farahani)	2/1/0/0
Satellite Geodesy Observation Techniques (Tourian, Douch)	2/1/0/0
Statistical Inference (Tourian, Douch)	2/1/0/0

Institute of Navigation

Breitscheidstraße 2
D-70174 Stuttgart
Tel.: +49 711 685 83400
Fax: +49 711 685 82755
ins@nav.uni-stuttgart.de
http://www.nav.uni-stuttgart.de

Head of Institute

Prof. Dr.techn. Thomas Hobiger

Deputy:	Dr.-Ing. Aloysius Wehr
Secretary:	Helga Mehrbrodt
Retired Professor:	Prof.i.R. Dr.-Ing. Alfred Kleusberg

Academic Staff

Dipl.-Ing. Doris Becker	Navigation Systems
Dipl.-Geogr. Thomas Gauger	GIS Modelling and Mapping
M.Sc. Kevin Gutsche	Precise orbit determination
Dr. Tomasz Hadas	GNSS troposphere
M.Sc. Shengping He	GNSS troposphere & PPP
M.Sc. Tomke Jantje Lambertus	Parameter Estimation in Dynamic Systems
M.Sc. Clemens Sonnleitner	Autonomous flight, ADS-B
Dipl.-Ing. (FH) Martin Thomas	Digital Electronics and Hardware Programming
M.Sc. Thomas Topp	Navigation Software Development
M.Sc. Arunprasad Vijayaraghavan	Hardware and FPGA programming
M.Sc. Rui Wang	GNSS, RTK, integrity
Dr.-Ing. Aloysius Wehr	Optical and Wireless Communication

IT

Regine Schlothan	Computer infrastructure and programming

Electronic Lab and Precision Mechanical Workshop (ZLW)

Dr.-Ing. Aloysius Wehr	Head of ZLW
Michael Pfeiffer	Mechanician Master
Sebastian Schneider	Electrician
Dipl.-Ing. (FH) Martin Thomas	Electrical engineer

External Teaching Staff

Hon. Prof. Dr.-Ing. Hans Martin Braun	RST Raumfahrt SystemtechnikAG, St.Gallen
Dipl.-Ing. Steffen Bolenz	Stadtmessungsamt, Stuttgart
Dr.-Ing. Werner Enderle	ESA / ESOC

Preface

This report summarizes the activities of the Institute of Navigation (INS) in the year 2020. We are happy that we could welcome three new PhD students, who have started work on different research projects and already cooperate with partners from industry. Research highlights, which are also described in greater detail in this report, are definitely our involvement in the establishment of the university's test area for autonomous flight, the use of GNSS for routine weather prediction and the development of a flexible, easy-to-use and extendable software framework that will serve the institute in the coming years in different research and student projects. Despite the challenges that came with the COVID-19 outbreak in the first quarter of the year, we were able to adopt quickly to the new circumstances and provide the content from all our lectures and exercises in different digital formats. Also, supervision of bachelor and master thesis projects could continue, though special measures for lab attendance had to be made in order to follow the hygiene rules set out by the university. As business travel came to an almost complete stop, we were not able to present our results on national and international conferences and had to hold almost all of our internal and external meetings in the form of teleconferences. This preface also serves the purpose to thank all staff of the INS for their strong support, flexibility and high motivation to carry the institute through the Corona year of 2020!

Research

The INS identifies new fields of applications, develops and tests navigation solutions and assigns research projects according to four "focus areas" which were defined in 2018. Figure 19 depicts those areas which are grouped around the topics of "positioning, navigation and timing".

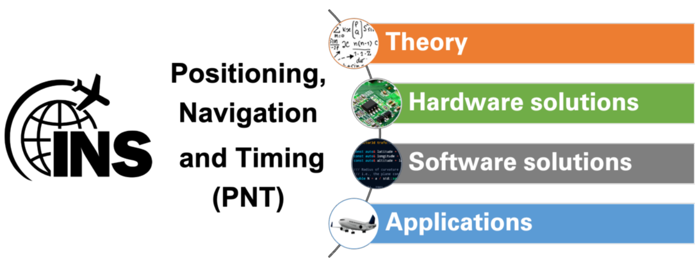

Figure 19: INS focus areas to which the institute is actively contributing with research projects.

While most of the current research projects can be clearly assigned to one or two focus areas shown in the figure, larger research projects, like AREA-BW or AutoCOM, described later in this report, are usually falling under the category "applications" but require intense input from the other three research areas. In the following, the purpose and vision for each research area is presented together with examples of ongoing research projects.

Research focus: Theory

The research area "Theory" involves the investigation and testing of mathematical models in order to improve existing positioning and navigation methods. The adaptation of classical parameter estimation methods and the development of new mathematical algorithms are key elements for innovative navigation applications. In this context the main focus lies on the realization of real-time solutions in order to facilitate mobile navigation applications (e.g. smartphones) or enable highly precise and accurate applications for operation of unmanned vehicles. Investigations concerning the optimal weighting of measurements and statistics-based fusion of sensor arrays are also a field of research. In addition, non-linear systems and their peculiarities are studied as well. The research output from this focus area is a precursor to other research topics but it also benefits from feedback from application-oriented fields of research.

Massive parallel particle filter algorithms

As one of its research focus, the INS has identified the topic of modern dynamic non-linear parameter estimation methods for autonomous navigation applications. Significant improvements in positioning, navigation and timing (PNT) concerning precision, accuracy, integrity, and availability over the last century have enabled a manifold of applications that are part of our daily life. In recent years the requirements of autonomous navigation have led to several challenges that need to be addressed to realize such ground-breaking concepts for aircraft, ship and land vehicle navigation. Most classical estimators rely on the idea that observations errors are following Gaussian normal distributions and third and higher-order moments of the probability distributions are zero. However, as this might not be totally correct for real-world sensors, one faces the challenge to determine the "most likely" state of a navigation system under the consideration of the real stochastic properties. Moreover, the solution space could be bounded or limited to given sets within the mathematical spaces of real or natural numbers. In most standard navigation applications, the extended Kalmanfilter (EKF) is used as it is simple to implement and yields acceptable results. Nevertheless, the EKF relies on a Gaussian white noise distribution in the prediction and update steps which would ensure that the Kalman filter yields a near-optimal solution. Furthermore, one needs to have exact knowledge about the dynamic state-space model and its stochastic properties and their time evolution need to be well understood. In reality, navigation applications are more complex and will typically include non-linear systems and measurements which do not necessarily follow a Gaussian normal distribution.

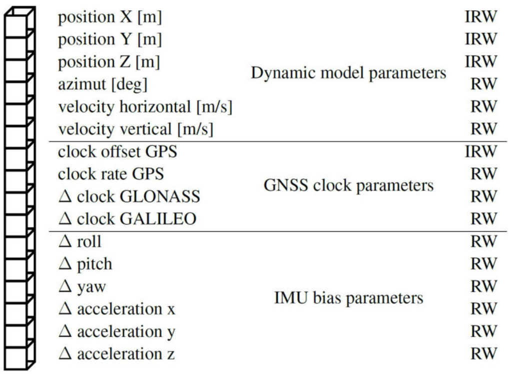

Figure 20: State vector parameters of a particle for a moving vehicle when using GNSS and IMU observations. The process model of these parameters is indicated by IRW (integrated random walk) or RW (random walk).

The EKF uses a linearization around the mean of the current state, and hence, the original problem is transformed into an approximative problem and solved such that it does not have to be the optimal solution of the original problem. The linearization can deteriorate the accuracy of the obtained solution or even lead to the divergence of the solution. In our research project, we focus on particle filters which can be considered as an alternative approach when reflecting on the aforementioned issues. The particle filter belongs to the group of Bayesian filtering techniques and it does not necessarily require the knowledge of the stochastic properties in advance. Hence, it is also suitable for nonlinear problems having measurements with non-Gaussian distributions, because it preserves the nonlinear structure of the problem. The basic idea of this filter is to create a set of particles where each particle represents a possible realization of the state vector which is assigned a weight. In each epoch, the states of particles are predicted based on their process model (see Figure 20). If measurements are available, the weight of each particle is recomputed, leading to an update of the PDF based on the residuals between observed and computed measurements. A major drawback of the particle filter is its computational cost which makes it difficult to process a large particle cloud. However, particle cloud processing is well suited for parallelization. To speed up the processing we use a graphics processing unit (GPU) to run the particle filter algorithms on a commercial of-the-shelf computing platform. The implementation of the algorithm is outlined in Figure 21. At every epoch, observational data are obtained and preprocessed on the CPU. Such data are then sent to the GPU where the main steps of the particle filter are performed using multiple threads. After each step, the main information, i.e. the estimated mean state and its stochastic properties are returned to the CPU. The particle filter program is written in C++ and will be part of the INSTINCT software which is described in greater detail the Software development section.

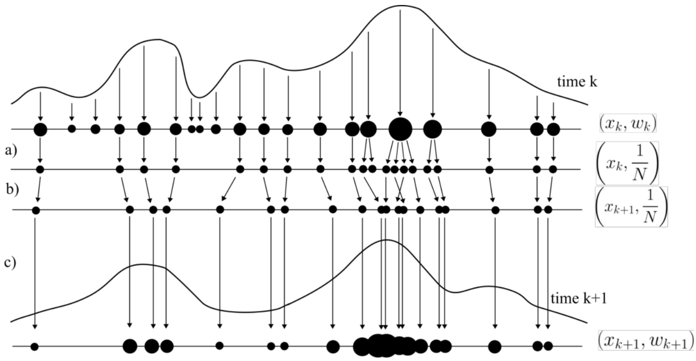

Figure 21: Schematic illustration of an 1D particle filter with N particles where x is the state vector of one particle and w its weight at time t.

Exchange training program at the University of Wrocław, Poland

From February to March 2020 one of our PhD students joined the PROM Programm at the Institute of Geodesy and Geoinformatics, Wrocław University of Science and Technology in Poland. The PROM program aims to support exchanges of PhD candidates and academic staff programs.

Wrocław University of Science and Technology

This program aims at increasing the competences and qualifications of PhD students. The funding is provided by the Polish National Agency for Academic Exchange. The host institute has vast experience in GNSS observation processing, precise point positioning, orbit determination (ILRS Associate Analysis Center), and especially in atmosphere modeling and parameter estimation. During her stay, our PhD candidate got notable support in terms of real-time GNSS parameter correction models. During this traineeship, GNSS observation correction models were tested and implemented in a GNSS Software developed at the INS. In addition, the BKG Ntrip Client (BNC) was added to the software suite. In particular, BNC was used to generate orbit and clock corrections so that they can be used together with broadcast ephemeris. The purpose of this exchange stay was to improve programming skills in C++, implement additional GNSS observations correction models in the GNSS Software, and to work with different real-time correction approaches for GNSS positioning and navigation.

Research focus: Hardware development

The combination of different sensor elements is a crucial approach when designing optimal navigation solutions for safety-critical and highly precise applications. Beside inertial navigation systems and GNSS the usage of novel sensors is therefor examined. Together with results from fundamental research and input from industry, new navigation instruments and sensors are developed and tested for their positioning and navigation abilities on different platforms. The use of software-defined-radio solutions reduces development costs and time and provides realistic estimates of the performance of an instrument that will be later realized in hardware or by the help of field-programmable gate arrays (FPGAs).

ADS-B

One of the research topics at the Institute of Navigation deals with Automatic Dependent Surveillance - Broadcast (short: "ADS-B"). In 2020 a low-cost receiver has been mounted on the roof of the building to monitor the airspace around Stuttgart. Airplanes up to a distance of approximately 120 km can be tracked with this receiver. It was for instance possible to monitor how air traffic declined as a result of the SARS-CoV-2 outbreak. Additionally, preparations for the installation of an high-grade ADS-B receiver from Thales have been made. This system is planned to be installed in Mengen at the "Testfeld eFliegen BW" (see section on page 67) at the end of 2021.

Figure 22: ADS-B antenna on the roof of the building of the institutes building.

One master thesis that dealt with the development of a software-defined ADS-B receiver and one bachelor thesis in which the student investigated the achievable precision of a multilateration ground station networks have been supervised in relation to ADS-B. On a long-term perspective, a network of several ADS-B base stations will be established and the obtained multilateration data shall be fused with the informations from the ADS-B messages. Thereby, it is expected that air traffic monitoring (ATM) will be significantly enhanced concerning reliability, robustness and integrity when using ADS-B, which has less initial and operational costs than traditional ATM systems.

Sensors for an alarm system against drowning in a bathtub

This project was initiated by the company Horcher and has been supported by the Central Innovation Programme for small and medium-sized enterprises (SMEs). The project's objective is the development of a system preventing people from drowning in a bathtub as used e.g. by nursing homes for the elderly. Project partners are company Horcher, Institute of Navigation (INS) and the German Institutes of Textile and Fiber Research (DITF). INS was assigned the task to develop and realize the sensor system, which comprises MEMS-Inertial Measurement Units (MEMS-IMUs), air pressure sensors, humidity sensors and an Indoor Microwave Positioning and Data Transmission System (IMPDS). The sensors and the transmitters of IMPDS are mounted on the patient's body. Therefore, the electronic components are developed in close cooperation with DITF regarding the requirements of so-called wearable electronics. In the year 2020, first experiments that considered dipping into water were carried out for evaluating the sensor performance and this study the situation when a body is drowning under water. The experimental setup for automatic testing is shown in Figure 23a.

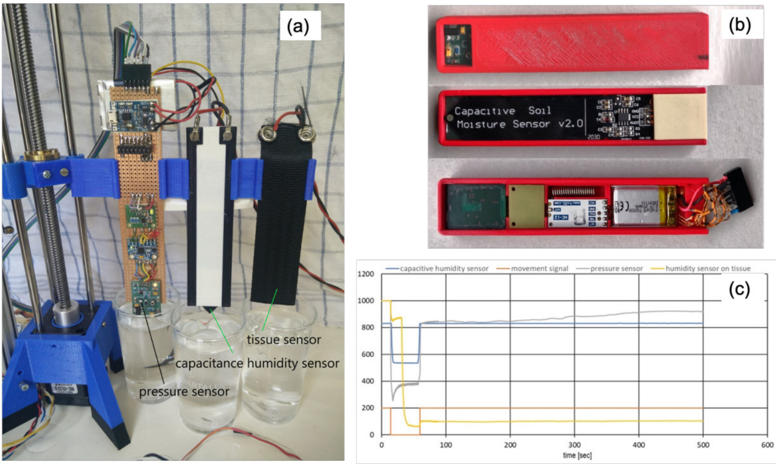

Figure 23: (a) Experimental setup for comparison of different sensors. (b) Demonstration sensor block (upper picture: opening pressure sensor, covered IMU, middle picture: humidity sensor, bottom picture: removed humidity sensor: IMU, transmitter and battery pack). (c) Comparison of different sensors.

The measurement results are plotted in Figure 23c. The red line (movement signal) depicts the position of the sensors. A value of 200 indicated that the object would be out of the water while a value 0 means complete drowning under water. The commercially available capacitance humidity sensor is functioning very precise and fast. Also the pressure sensor shows clearly, when a body goes under water. The diagram makes clear that there is a certain recovery process, if the sensor is out of water. But this feature does not effect the decision, if the body is under water. The humidity sensor on the tissue reacts differently and tests reveals that a clear signal can be obtained with a delay of a 14 sec. The tissue requires more than an hour to become dry which is the requirement to report back the initial zero value. On the basis of this experiment a demonstration sensor block was realized comprising a six degree of freedom inertial measurement unit LSM6DSOX from STMicroelectronics, a pressure sensor DPS368 from Infineon, a humidity sensor and a wireless data link which connects to a central computer. All items were mounted in a compact housing and were powered by a small battery pack (see Figure 23b). Software was implemented for data gathering and transmission in parallel to the electronics development and mechanical setup work. Special emphasis was put on the development of a wearable patch antenna. Here, analytical experiments were carried out concerning the determination of the relative dielectric constant of the used glue fixing for the antenna foil on the backing material. Figure 24 depicts the principle measurement setup.

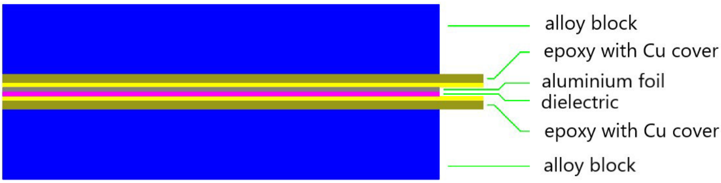

Figure 24: Principle measurement setup for determining dielectric constant

Six foils were studied. The foils had got the physical dimensions 100 mm x 100 mm. According to Table 1 they exhibit different thicknesses of the dielectric material which later will be applied as glue.

Sample	thickness (μm)	solid content (%)
1	100	45
2	200	45
3	300	45
4	100	13.5
5	200	13.5
6	300	13.5

Table 1: Thickness of the studied dielectric material

Figure 25a shows the determined values of the relative permeability as a function of frequency. On the basis of this values a patch antenna (see Figure 25b) can be dimensioned, now.

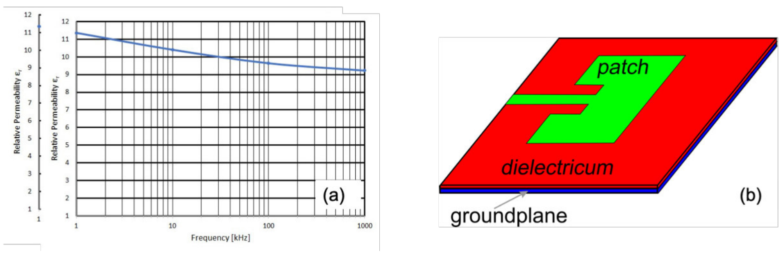

Figure 25: (a) Relative permeability as function of frequency. (b) Patch antenna.

Research focus: Software development

In order to test new algorithms and navigation solutions the institute has started to develop its own software toolchain. All code is based on modern C++ language, optimized for run-time performance while still being simple enough so that navigation software solutions can be easily designed by drag-and-drop style. Thus, the software is usable by non-experts, who have only very little knowledge about the implemented algorithms but need robust and precise navigation solutions, as well as navigation professionals, who adopt the software for their particular need or extend it with new modules to realize new and innovate solutions. Therefore, easy testing and verification of improved algorithms and models for positioning and navigation of static and moving objects is possible. The software development efforts are complemented by studying systematic effects, which set an implicit limit for improving the accuracy of positioning solutions.

INSTINCT - INS Toolkit for Integrated Navigation Concepts and Training

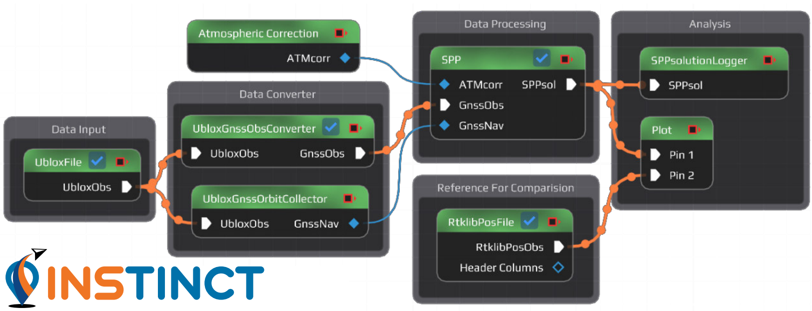

Figure 26: INSTINCT dataflow for a SPP algorithm.

INSTINCT is a software framework written in modern C++ which provides a GUI to design navigation algorithms (Figure 26). The software bases on a node-based approach which follows the data-flow programming paradigm. This means, that functionality which serves the same purpose, like reading a file or sensor, is bundled into a node. These nodes are self-contained and do not know about the functionality of other nodes, which makes it very easy to understand, use and extend them. The only way how nodes exchange information is by their input and output pins. These pins can have different types, ranging from static objects (blue diamond pins in Figure 26) to dynamic data (white arrow pins), which is for example sent every time a new sensor measurement is available. To connect pins, and therefore determine where the data should be passed to, links can be created by drag-and-drop between the node pins. Every time data is passed over these links, an animation (orange dots in Figure 26) is triggered in order to help the user understand the data-flow by such a visual aid. A major advantage of this node-based approach with predefined interfaces is, that it is easy to replace data sources, e.g. switch from an input file to a real sensor node. Therefore flows can be tested with recorded

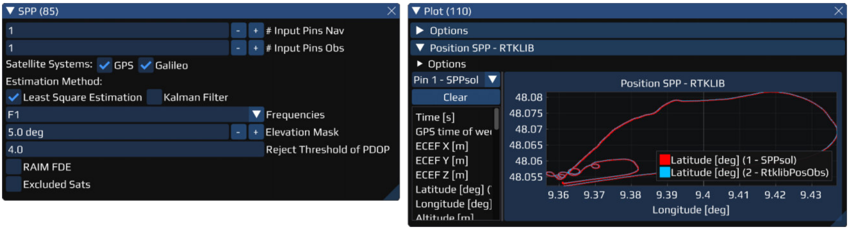

Figure 27: Config windows for the SPP node, where parameters can be adapted and the Plot node, where data can be visualized.

data and then only one node needs to be exchanged to utilize the exact same structure in a real-time scenario. With this simplicity it is easy to create a data-flow and visualize the results. Moreover, it is possible to use the exact same data-flow and run the program without the GUI on e.g. a single-board computer like a Raspberry Pi. This then achieves great performance while using the already tested data-flow without any reconfiguration.

The core of each node is a configuration window where data can be visualized (Figure 27) or parameters can be adjusted on-the-fly. This enables the user to adjust his algorithms and directly see the effects which is much faster than editing setting files, restarting the program and then plotting the data in other tools. The configuration windows are designed with an open source Immediate Mode GUI library which allows the more advanced user to fully customize his own nodes to his needs. INSTINCT is meant to be used for research projects, training and also for real-time vehicle navigation. Researchers can implement their own algorithms inside new nodes and take advantage of a large set of already available functionality. This enables them to focus on the research instead of implementing fundamental things over and over again. Students at universities or trainees in companies can use the simple user interface to experiment with navigation algorithms and see how different parameters affect the solution. This provides a more practical and deeper learning experience. Finally the software can be used to provide an on-board real-time navigation solution which is customized to the available hardware and mission needs. Therefore it delivers the maximum performance while still being adaptable to future changes.

PODCAST - Precise Orbit Determination for Cutting-edge Adaptive Satellite Technology

PODCAST is a C++ software that is developed at the Institute of Navigation in cooperation with Airbus. The development started in November 2020 and is within the project AutoCom co-funded by the German Aerospace Center (DLR) and Airbus. The software aims to provide Precise Orbit Determination (POD) capabilities for future satellite missions while enabling research activities in its development. The need for POD arises in particular from the requirement of very precise position information in order to acquire high-quality Synthetic-Aperture Radar (SAR) images or altimetry measurements. PODCAST is developed with the goal to provide a

POD solution for the ground segment to enable high-quality data in the post-processing of these images and measurements.

PODCAST will implement established concepts of Precise Orbit Determination for non-agile LEO satellites. A further goal of this software is to enable the analysis of the influence of agility and low-thrust station keeping on POD algorithms and how this affects the accuracies of the final estimation. Ultimately, PODCAST shall provide a POD solution for agile satellite missions, which currently does not exist on the market. In a first step, the framework of PODCAST has been set and first estimations with simulated observations have been performed. The software will be subsequently improved to incorporate additional observations and dynamics to reach the required estimation accuracy requirements. From this validated software for POD of non-agile satellites, further work will be done to ultimately provide a software for POD of non-agile as well as agile satellites. The software will be extensively validated with hardware-based and software-based GNSS simulators, real hardware and realistic mission scenarios.

Research focus: Applications

Research and development is either driven by the demand for certain solutions or applications. However, it might also happen that particular unintended applications emerge from research as it turns out that the theoretical foundations of soft- and hardware solutions also serve another purpose. One example for such an application is GNSS meteorology, which allows to derive crucial parameters of the troposphere from GNSS measurements. Thus, atmospheric delay, which is usually an error source that needs to be mitigated carefully when processing GNSS observations for the purpose of positioning and navigation, becomes a valuable source of information, when extracted properly within the parameter estimation process. The next sub-section discusses some recent findings that relate to such an undertaking. On the other side, the institute's involvement in a large research infrastructure for autonomous flight operations, as described in the second sub-section, can be seen an incubator for new applications that will emerge when research projects related to safe, precise and reliable navigation of unmanned air vehicles are carried out.

GNSS meteorology

The H2020 project "Real-Time GNSS for European Troposphere Delay Model" (ReS4ToM) aims to develop a high quality real-time GNSS model of the troposphere delay for Europe (`https://cordis.europa.eu/project/id/835997/en`). It will combine in a consistent and operational way multiple novel aspects of GNSS data processing in real-time, e.g. undifferenced and uncombined multi-GNSS data processing, estimation of horizontal gradients, optimized stochastic modeling and robust outlier detection in real-time. In [Hadas et al.(2020)] , the impact of Precise Point Positioning (PPP) processing parameters on estimated tropospheric products is investigated. It is noticed, that a multi-GNSS solution, with proper intersystem weighting, reduces the a posteriori standard deviation of estimated Zenith Total Delay (ZTD) by up to 37 %. The estimation of real-time gradients improves height precision by 27 % on average and can significantly affect ZTD estimates. Real-time gradients are estimated with an uncertainty of 0.1 mm to 0.3 mm, but their accuracy with respect to an NWP model or post-processing results is not investigated in this study. An advanced strategy for real-time troposphere monitoring is proposed, which is superior to the common approach, i.e. it has 0.9 % more results over the entire year 2019, and the a posteriori error of estimated ZTD is reduced by 41 % on average. The accuracy with respect to the final ZTD product from the International GNSS Service (IGS) improves by 17 % and varies over stations from 5.4 to 10.1 mm (Figure 28). Such performance will legitimate real-time ZTD estimates for assimilation into NWP.

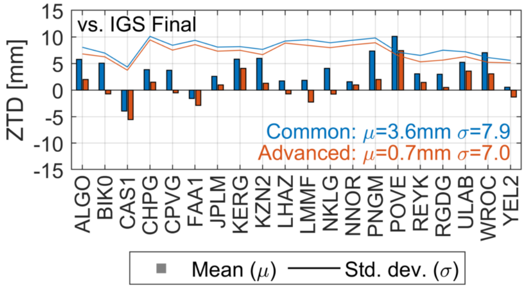

Figure 28: Comparison of real-time ZTD obtained with common and advanced strategy against IGS Final product.

In [Hadas and Hobiger(2020)], it is demonstrated, that Galileo and supporting services are already mature enough to provide a reliable information on troposphere state in real-time. However, the performance of Galileo-only solution is still not as good as of GPS-only solution in terms of continuous performance, standard deviation of estimated ZTD and accuracy with respect to final products. On the other hand, a combined GPS+Galileo solution can be achieved in real-time without a lot of extra effort, which leads to significantly better results than a GPS-only solution. Processing of nearly twice as much observations in the combined solution leads to the decrease of a ZTD standard deviation by a factor of 1.5 to 2.0. The accuracy with respect to final products improves by 3.7 % to 8.5 %. For IGS stations, the accuracy is 8.0 mm and 6.5 mm with respect to USNO and CODE products, respectively. For European Permanent Network (EPN) stations, the accuracy is 5.4 mm and 5.0 mm with respect to BKG and MUT solutions, respectively. Finally yet importantly, the spectral analysis of real-time ZTD from GPS-only, Galileo-only and GPS+Galileo solution reveals further advantages of using the combined solution. Whereas single system ZTD products suffer from orbit related artificial signals of high frequency, the combined GPS+Galileo solution suppress such effects. Thus, a combined GPS+Galileo solution is expected to be not only more available over an average day, but the solution itself will be more precise and accurate and is therefore definitely preferable to a GPS-only product when it comes to assimilation of GNSS ZTD in NRT numerical weather models.

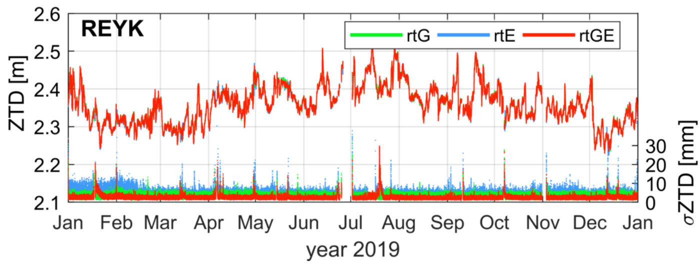

Figure 29: Time series of real-time ZTD for station REYK.

Testfeld eFliegen BW

The INS is one of the institutes of the University of Stuttgart that is building up the "Testfeld für energieeffizientes, elektrisches und autonomes Fliegen" (short: "Testfeld eFliegen BW") together with partners from industry under the lead of the IfR (www.ifr.uni-stuttgart.de). In the year 2020 the partners founded the association "AREA B.W." which will manage and operate the project and the two test sites in Mengen and Lahr and represent its members. Furthermore the association provides a framework for usage regulations that apply to the test site and which provide simple access to generic take-off permits.

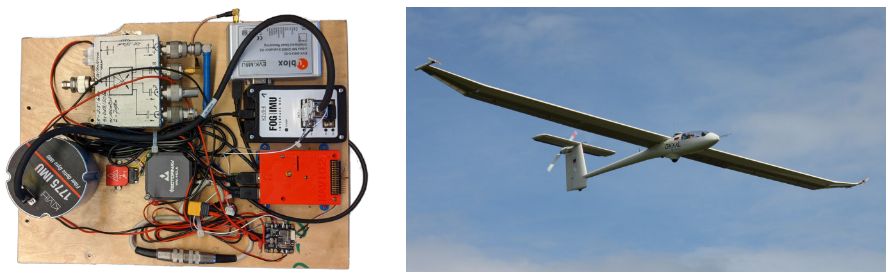

Figure 30: Research activities of the INS together with other institutes of the University of Stuttgart on the "Testfeld eFliegen BW": Platform with the different IMU and GNSS sensors (left); Icaré during flight with visible GNSS antenna behind the cockpit (right).

Besides the acquisition of different aeronautic and navigation infrastructure for autonomous flying (see e.g. section) which can be used by partners and external parties, which are interested in testing their equipment, first flight test have been performed. In one of these test, the INS equipped the electric solar aircraft Icaré of the IFB (www.ifb.uni-stuttgart.de) with a set of low- and high-grade navigation sensors (see Figure 30). Thus the institute collected data from different IMUs and GNSS sensors for comparison and investigation of reliable, high accuracy sensor fusing algorithms for Urban Air Mobility (UAM) vehicles and autonomous drones.

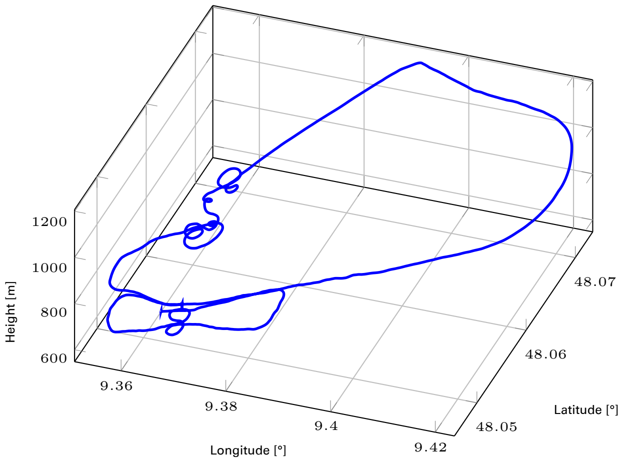

Figure 31: Flight trajectory of one of the performed flights

List of Publications

[Klopotek et al.(2020)] Klopotek G., T. Hobiger, R. Haas and T. Otsubo: Geodetic VLBI for precise orbit determination of Earth satellites: a simulation study, Journal of Geodesy, Vol. 91, Iss. 52, `https://doi.org/10.1007/s00190-020-01381-9`, 2020.

[Hadas et al.(2020)] Hadaś T., T. Hobiger and P. Hodryniec: Considering different recent advancements in GNSS on real-time zenith troposphere estimates, GPS Solutions, Vol. 24 No. 99, pp. 1-14. `https://doi.org/10.1007/s10291-020-01014-w`, 2020.

[Hadas and Hobiger(2020)] Hadaś T. and T. Hobiger: Benefits of Using Galileo for Real-Time GNSS Meteorology, IEEE Geoscience and Remote Sensing Letters, pp. 1-5, `https://ieeexplore.ieee.org/document/9141353`, 2020.

[Nievinski (2020)] Nievinski F., T. Hobiger, R. Haas, W. Liu, J. Strandberg, S. Tabibi, S. Vey, S. Williams and J. Wickert: SNR-based GNSS reflectometry for coastal sea-level altimetry – Results from the first IAG inter-comparison campaign, Journal of Geodesy, vol. 94, iss. 70, `https://doi.org/10.1007/s00190-020-01387-3`, 2020.

List of Presentations

[Hobiger(2020)] Hobiger T., Navigation of autonomous airplanes: Geodetic Colloqium at the University of Hannover, Jan. 21, 2020.

[Hadas and Hobiger(2020)] Hadaś T. and T. Hobiger: Contribution of Galileo to real-time GNSS meteorology, International Workshop on Improving GNSS and SAR Tropospheric Products for Meteorology, Feb. 25-26, 2020.

Teaching and Supervision

The university's regulations due to the COVID-19 pandemic made it necessary to adopt all course content of the summer semester 2020 as well as the winter semester 2020/21 into digital formats. Thus, all lectures had to be filmed and were then provided to the students so that they could attend classes virtually according to their own schedule and pace. Both classroom recordings as well as screencasts with a drawing tablet were provided in order to maximize the learning outcomes, i.e. the specific knowledge, practical skills, areas of professional development, attitudes, or higher-order thinking skills which are expected from students to develop, learn, or master by the end of the particular course. Supervision of bachelor and master thesis projects had to be set into a digital format as well. Some graduate projects which required lab attendance could be organized under consideration of hygiene concepts und special preparations. So, the new software-defined radio LimeSDR funded by the study commission, could be programmed and evaluated in the lab as part of a study about simulation of GNSS jamming attacks. (Figure 32)

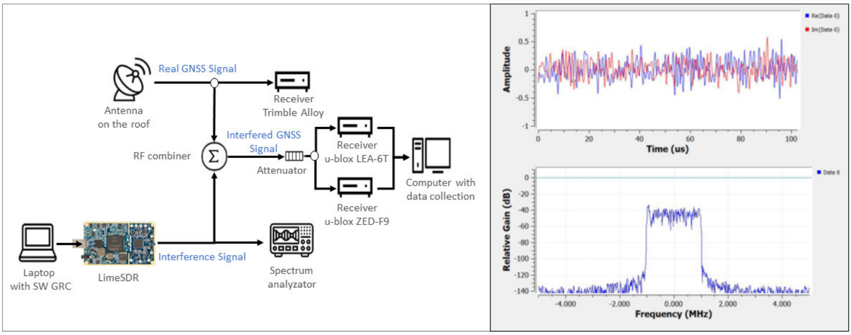

Figure 32: Work flow of the jamming simulation experiment (left) and generated White Gaussian Noise jamming signal (right)

With the purchase of an RC car (Figure 33), remodeling and equipment of GNSS and inertial sensors the institute has now a platform which allows students to test real-time positioning and navigation concepts in different courses and student projects. The RC car has been successfully included into the field work project at the end of the summer semester and one master thesis has been already been completed, dealing with sensor fusion on that platform.

Figure 33: The institute's RC car which has been equipped with electronic for autonomous driving

The following parts of this section list student thesis projects which were completed in 2020 and summarize the teaching activities of the institute.

Bachelor Theses

Ernst, Johannes: Robuste Cycle-Slip Detektion bei GNSS Messungen (Supervisor: T. Lambertus)

Blei, Torben: Doppler-bedingte GPS Code Interferenzen (Supervisor: D. Becker)

Helfert, Carsten: Genauigkeitssimulation von Multilaterations-Bodenstationsnetzwerken (Supervisor: C. Sonnleitner, T. Hobiger)

Master Theses

Duan, Yongxu: Temperature dependency of a low-cost IMU (Supervisor: C. Sonnleitner, T. Hobiger)

Hem, Shengping: Development of a software-defined ADS-B receiver (Supervisor: C. Sonnleitner, T. Hobiger)

Jiang, Zhenbing: ARAIM – Implementierung eines aktuellen Algorithmus (Supervisor: D. Becker)

Jilani, Muhammad Irfan Haider: Impact of Non-Linearity on IMU/GNSS Sensor Fusion Comparing Different State Estimation Approaches (Supervisor: T. Hobiger, T. Topp)

Wei, Yazheng: Track Verification of Smartphone Users (Supervisor: T. Hobiger, V. Renaudin (IFSTTAR))

Xin, Jie: Analyse der GNSS Integrität mittels Stanford-Diagramm (Supervisor: D. Becker)

Yang, Xiaoheng: Development of a simulator for GNSS jamming attacks (Supervisor: D. Becker)

Zhang, Chanjuan: Accuracy Assessment of Kinematic Precise Point Positioning with Triple GNSS Constellation (Supervisor: T. Hobiger, M. Naeimi (Bosch))

Activities in National and International Organizations

Prof. Hobiger Editorial board member "Journal of Geodesy"
Editorial board member "Earth, Planets and Space"
Editorial board member "Acta Geodaetica et Geophysica"
Member of the German Geodetic Commission
Corresponding member of the Austrian Geodetic Commission
Fellow of the International Association of the Geodesy
Member of the Institute of Navigation
Member of the Royal Institute of Navigation
Member of the German Institute of Navigation
Member of the American Geophysical Union

Prof. Kleusberg Fellow of the International Association of the Geodesy
Member of the Institute of Navigation
Member of the Royal Institute of Navigation
Member of the German Institute of Navigation

Mr. Gauger Member of VDI/DIN KRdL working group on Deposition parameters [NA 134-02-01-08 UA]
Member of ICP Forests
Member / Guest scientist of Bund-Länder-Fachgespäch Stickstoffdeposition (FGN)
Member of StickstoffBW, AG1 Deposition

Education - Lectures/Exercises

Bachelor Geodesy & Geoinformatics

Adjustment Theory I (Hobiger, Lambertus)	2/1
Adjustment Theory II (Hobiger, Lambertus)	2/1
Fundamentals of Navigation (Hobiger, Wang)	2/2
Integrated Fieldwork (Lambertus, Sonnleitner)	2/10 days
Introduction of Geodesy and Geoinformatic (Hobiger, Becker)	2/2
Measurement Techniques II (Wehr) 2/2	

Master Geodesy & Geoinformatics

Inertial Navigation (Hobiger, Sonnleitner)	2/1
Integrated Navigation (Hobiger, Sonnleitne)	2/1
Interplanetary Trajectories (Becker)	2/2
Measurement Techniques in Navigation (Wehr)	1/3
Navigation of Air and Surface Vehicles (Becker)	2/1
Parameter Estimation in Dynamic Systems (Hobiger, Lambertus)	2/1
Radar Measurement Methods I (Braun)	1/1

Radar Measurement Methods II (Braun)	1/1
Selected Chapters of Navigation (Enderle)	2/0

Master GeoEngine

Dynamic System Estimation (Hobiger, Lambertus)	2/1
Integrated Positioning and Navigation (Hobiger, Sonnleitner)	2/1
Satellite Navigation (Hobiger, Wang)	2/1

Master Aerospace Engineering

Inertial Navigation (Hobiger)	2/0
Satellite Navigation (Hobiger)	2/0

Master Electromobility

Navigation of Surface Vehicles (Becker)	2/0
Satellite Navigation (Hobiger)	2/0

Institute for Photogrammetry

Geschwister-Scholl-Str. 24D
D-70174 Stuttgart
Tel.: +49 711 685 83336
Fax: +49 711 685 83297
info@ifp.uni-stuttgart.de
`http://www.ifp.uni-stuttgart.de`

Head of Institute

Prof. Dr.-Ing. Uwe Sörgel

Deputy:	apl. Prof. Dr.-Ing. Norbert Haala
Personal Assistants:	Carmen Kaspar
	Ute Schinzel
Emeritus Professors:	Prof. Dr.-Ing. Dr. hc. mult. Fritz Ackermann
	Prof. Dr.-Ing. Dieter Fritsch

Academic Staff

M.Sc. Tobias Bolz	Object Reconstruction from SAR Images
Dr.-Ing. Michael Cramer	Photogrammetric Systems
Dipl.-Ing.(FH) Markus Englich	Laboratory, Computing Facilities
apl. Prof. Dr.-Ing. Norbert Haala	Photogrammetric Computer Vision
M.Sc. Lena Joachim	Integrative Computational Design
M.Sc. Michael Kölle	Crowd-based Data Collection
M.Sc. Dominik Laupheimer	Classification in Remote Sensing
M.Sc. Stefan Schmohl	Deep Learning in 3D Remote Sensing
M.Sc. Philipp Schneider	SAR Interferometrie
Dr.-Ing. Volker Walter	Geoinformatics

Stipendiaries and external PhD Students

M.Sc. Hasan Almassri	Localization and mapping (SLAM)
M.Sc. Stefan Cavegn	Image-based Mobile Mapping
M.Sc. Ke Gong	3D Reconstruction
Dipl.-Phys. Hendrik Schilling	Classification of Hyperspectral Data
M.Sc. Mehrdad Nekouei Shahraki	Photogrammetric Image Processing
M.Sc. David Skuddis	LiDAR-based Mobile Mapping
M.Sc. Wei Zhang	Visual SLAM for Augmented Reality
M.Sc. Xinlong Zhang	Object Recognition from LiDAR Data

External Teaching Staff

Dipl.-Ing. Stefan Dvorak, Amt für Stadtentwicklung und Vermessung, Reutlingen

Research Activities in ifp organized in four thematic Groups

Geoinformatics	Dr.-Ing. Volker Walter
Photogrammetric Computer Vision	apl. Prof. Dr.-Ing. Norbert Haala
Photogrammetric Systems	Dr.-Ing. Michael Cramer
Remote Sensing	Prof. Dr.-Ing. Uwe Sörgel

Research Projects

Crowd-based Active Learning for Semantic Segmentation of ALS Point Clouds

Supervised Machine Learning (ML) systems such as Convolutional Neural Networks (CNNs) are known for their great need for labeled training data. However, in case of geospatial data and especially in terms of Airborne Laserscanning (ALS) point clouds, labeled data is rather scarce, hindering the application of such systems for semantic segmentation.

Therefore, we rely on Active Learning (AL) for significantly reducing necessary labels. AL can be considered as a construct composed of three interdependent components: i) the ML model, ii) the strategy for selection of most informative points and iii) the employed oracle. The interaction of these components is depicted in Figure 1.

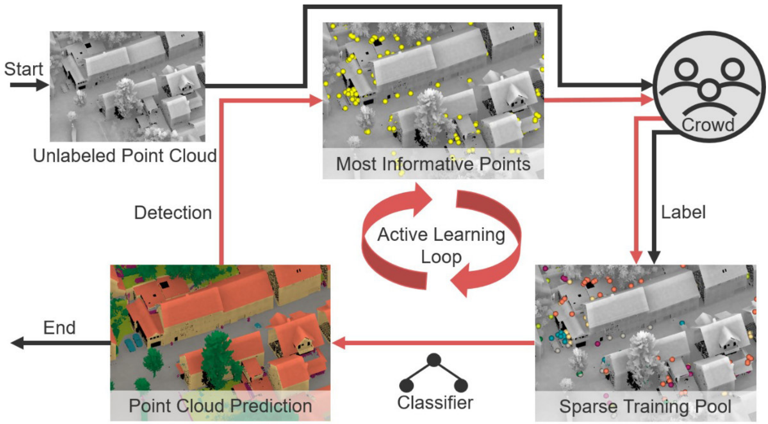

Figure 1: Crowd-based Active Learning pipeline for semantic segmentation of ALS point clouds.

We assume to have acquired an ALS point cloud and run basic post-measurement routines (e.g. alignment of strips). This dataset can be thought of as unlabeled training pool U. For initializing the AL loop, a first small training pool T is required including samples for the desired classes. T is built by the oracle, embodied by the crowd in our case. Based on T, we can train an arbitrary classifier for semantic segmentation of the point cloud. After inference of the trained model on the remaining training set R, the main objective in AL in each iteration step is to select those instances of R which have the greatest positive influence on the performance of the model and therefore justify manual labeling effort. Here, we aim on finding an intrinsic measure for determining the uncertainty of the model's predictions. One established method is to select those points where the entropy of respective a posteriori probabilities $p(c|x)$ that point x belongs to class c is maximum (i.e. the classifier is most uncertain about these points, see also Figure 1. Afterwards the selected points are presented to crowdworkers for labeling. This AL loop (denoted by red arrows in Figure 2) is repeated for n iteration steps until convergence or until exhaustion of budget. Thus, the ML model gradually improves in each iteration step by learning from the crowd in the sense of a human-in-the-loop system.

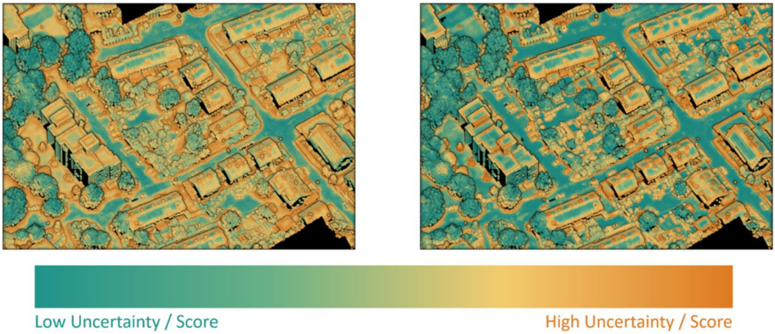

Figure 2: Derived point-wise entropy scores of the first iteration step (left) and the last iteration step (right). Color scale ranges from dark blue = low sampling priority to orange = high sampling priority. Points missing on the right were selected and added to T.

IntCDC: Environment Monitoring for a Cyber-Physical Construction Platform

The Cluster of Excellence IntCDC (Integrative Computational Design and Construction for Architecture) of the University of Stuttgart aims to rethink design, fabrication and construction in order to tackle the current challenges of the building industry, such as the lack of sustainability and productivity. IntCDC is funded by the German Research Foundation (DFG).

One of the research activities within this interdisciplinary project is the development of a cyber-physical construction platform, namely a tower crane, for automated on-site assembly of prefabricated building elements. In cooperation with the Institute for System Dynamics, we are developing the control for the automated tower crane and the corresponding monitoring system. The goal is to enable a fully automated load handling including the pick and place processes and the transportation in between. Therefore, task scheduling, path planning and an online feedback for collision avoidance during transportation are needed. That is why we developed a concept for a network of sensors, which will be placed at the crane itself and at the surrounding of the construction site.

The first configuration consists of cameras located at the boom of the crane (see Figure 3), which are taking overlapping images during the movement of the crane. Another component is a network of stereo cameras distributed around the site itself. The crane cameras will be mainly used to generate a digital surface model of the site as basis for path planning. The

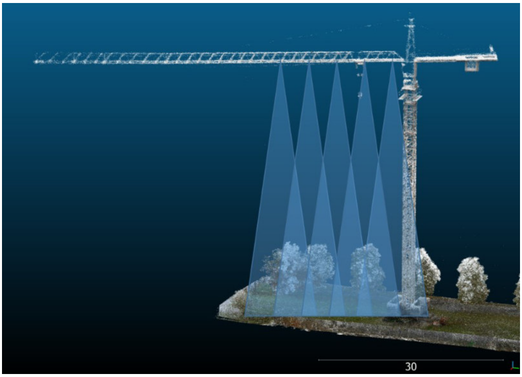

Figure 3: Point cloud of the IntCDC test site with the tower crane as part of a cyber-physical construction platform. The blue triangles show how the crane cameras will take overlapping images of the site.

stereo cameras will be mainly used to detect persons for collision avoidance during the transportation process. As these concepts are to be implemented and evaluated on a real tower crane at our IntCDC test site (see Figiure 3), the configuration of the communication between the crane control and the sensor system is also part of our research.

Extracting and evaluating Clusters in DInSAR Deformation Data on single Buildings

Beside ground-based techniques, remote sensing applications such as space-borne synthetic aperture radar (SAR) has developed to an acknowledged way to augment and prove terrestrial monitoring. Its ability to capture a wide area makes SAR a unique and valuable technique for urban building monitoring. Differential interferometric SAR (DInSAR) analysis of high-resolution X-Band data such as the TerraSAR-X satellite's is hereby able to measure deformations in the millimeter scale. The persistent scatterer interferometry (PSI) approach has developed to be a reliable and well understood method in urban deformation monitoring and is implemented in several software bundles. By analyzing a time series of coherent SAR images, PSI is able to derive the 3D position of persistent scatters and their overtime deformation, projected on the satellite's radial line-of-sight (LOS). In urban environments, these persistent scatterers (PS) are mainly caused by men-made structures since trihedral corners and metal parts are fostering the backscatter of radar signals. As others have shown, depending on the type of the facade, buildings in high resolution X-Band data can often have more than 1 PS per m^2 which leads to hundreds of points on small houses and can easily surmount thousands on large office buildings. The interpretation and visualization of such high number of points can be challenging. One often needs civil engineering experts to interpret the deformation patterns and link them to the actual construction process, therefore a simple representation and pre-analysis of those big numbers of time-series is necessary.

We combine OpenStreetMap (OSM) with DInSAR analysis to separate single buildings in order to find substructures in those instances. Identifying such substructure may help to understand the physical movement of a building and can point out rigid structures, which, in case of a monitoring, need to be measured individually. The analysis of substructure motions on a single building can help to detect potentially risky deformation patterns, i.e., if two adjoining parts of a building are moving in opposite directions. We are evaluating our findings with in-situ 3D tachymeter measurements and precise levelling to compare the deformation time series we derived from the satellite data.

In our experiments, we are using TerraSAR-X High Resolution Spotlight data acquired over Stuttgart, Germany during a time span of almost 3 years. The ground truth data are measured in the course of the ongoing construction of a new underground main station in the city center.

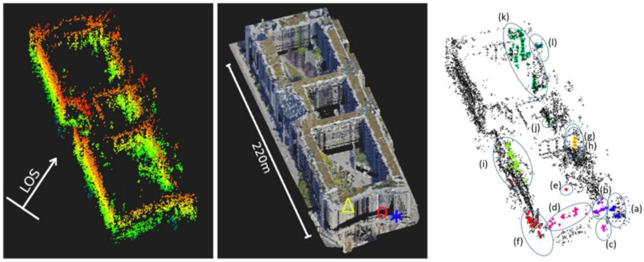

Figure 4: Left: 13000 PS Points on the building (Z-color-coded, segmented from OSM footprint). Middle: ALS point cloud of the building. The levelling points are marked by * and o. The corresponding time series are shown in Figure 5. Right: Distribution of clusters on a building. Each group and color indicates a different cluster. The related time series are shown in Figure 5.

Airborne (PolIn)SAR for coastal Protection

The Wadden Sea covers large areas of the North Sea coast in Germany, the Netherlands and Great Britain and is exposed to the influence of tides and storm surges. To ensure the safety of seafaring traffic and the protection of the coastal areas among other things, up to date high-resolution geodata is required. This data includes digital surface and terrain models, digital imagery and a variety of 3D line geometry such as water-land-boundaries or 3D structural lines.

The GeoWAM (www.geowam.net) Project investigates the possibility to replace state of the art laser scanning with airborne SAR. The use of SAR has some advantages, such as weather independence and larger strip width, but also comes with problems due to the specifics of the recording. Figure 6 shows the resulting DEM of the delayed flight campaign in the summer 2020. As part of the project the ifp focuses on the reconstruction of 3D structures to monitor dikes and other coastal protection buildings.

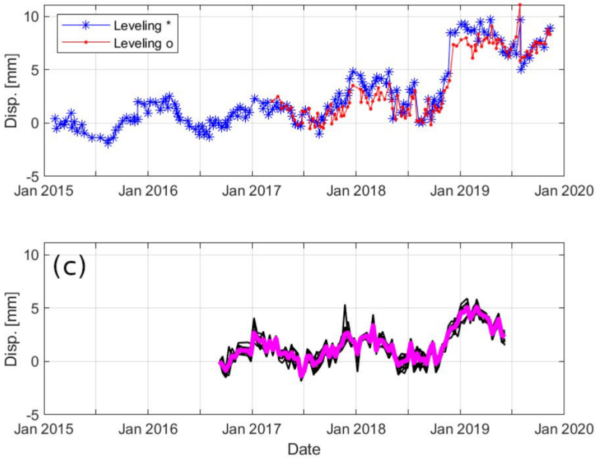

Figure 5: Top: Ground truth from two precise levelling points underneath the building (see Figure 4). Bottom: Deformation of the (spatially) closest PSI cluster (c) to the leveling points.

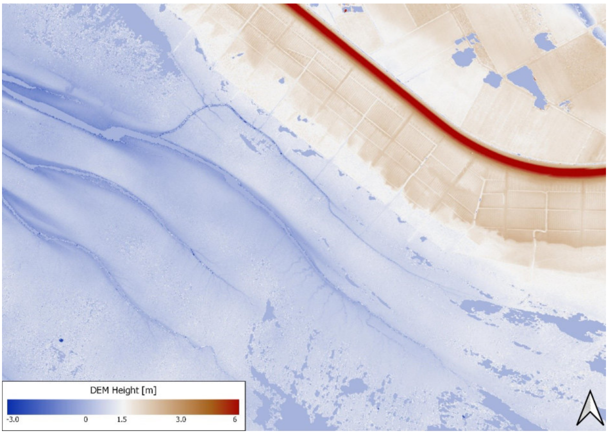

Figure 6: Interferometric DEM of the coastal area along the river Elbe close to Neufelderkoog, Germany.

State-of-the-art methods to extract structures designed for ALS input mostly rely on the high-resolution point clouds, which leads to the problem of them not working with SAR data. Using SAR data, two different basic inputs can be used. First the interferometric elevation model and secondly the raw SAR amplitude images. In the last year we developed a method based on the Touzi ratio-based edge detector for SAR images. In addition to a new computational method for very high-resolution SAR images an enhanced method for different sized windows was designed to tune the results for different structures. Figure 7 shows the results of the edge detector. The detection of Edge pixels is a crucial part of detecting and classifying 3D structures, but for an extraction this information needs to be post processed to generate vectors and then can be used for a classification.

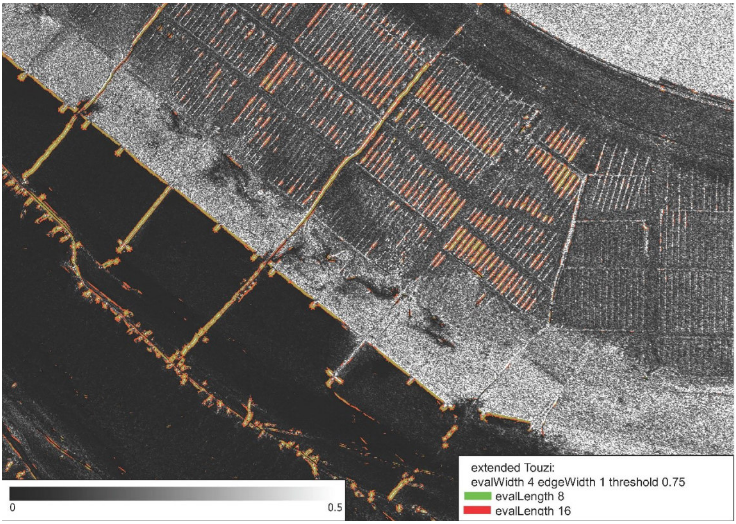

Figure 7: Results of the extended Touzi edge detector on the SAR amplitude image.

LiDAR Scan-Matching in Challenging Environments

The term scan matching describes the process of merging two or more LiDAR scans into a consistent scene. The process is often referred to as pointcloud registration. Scan matching is classically used where maps of the environment or models of objects are created using LiDAR sensors. Scan matching techniques are also used in robotics applications where a robot is moving through unknown environments or where the robot's own motion is to be computed.

Figure 8 shows an example of the merging of scans by scan matching. On the left side, three individual scans are shown in different colors to emphasize the composition of the scene from individual scans. On the right side, the same scene consisting of ten scans is shown.

Various scan matching algorithms have been developed over the past decades, and their goodness and robustness can vary greatly depending on the nature of the environment and sensor configuration. Some methods rely on structured environments to find suitable landmarks, while still other methods rely on good approximations during initialization to converge.

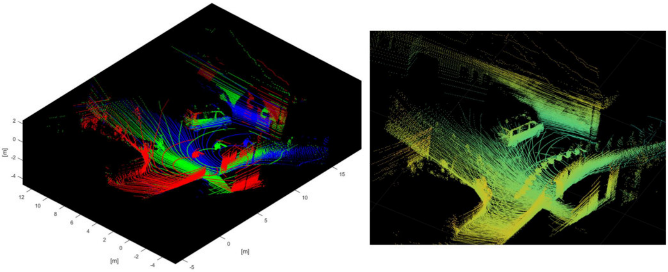

Figure 8: Left: Scene consisting of three matched LiDAR scans (red, green and blue). Right: Same scene consisting of ten matched LiDAR scans.

In this project, novel scan matching algorithms for mobile laser scanners are investigated and compared to known methods. The goal here is to identify suitable methods that can be used in the future for high-accuracy trajectory reconstruction of a mobile integrated sensor system in challenging environments. In addition to the LiDAR sensor, the sensor system is also equipped with a high-precision IMU and GNSS receivers. The goal of the project is to develop a system whose trajectory can be reconstructed and georeferenced even in very difficult environments where GNSS is temporarily unavailable.

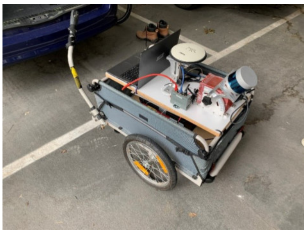

Figure 9: Integrated system with LiDAR scanner, GNSS receiver and high accuracy IMU.

Juggling With Representations: On the Information Transfer between Imagery, Point Clouds, and Meshes for Multi-Modal Semantics

The past decade has shown that 3D data acquisition and data processing has increasingly become feasible and important in the domain of photogrammetry and remote sensing. Hence, the automatic semantic segmentation of the huge amount of acquired geospatial data has become a crucial task. Images and point clouds are fundamental data representations for geospatial data, particularly in urban mapping applications. Textured 3D meshes intrinsically integrate both data representations geometrically by wiring the point cloud and texturing the surface elements with available high-resolution imagery (hybrid data storage). Furthermore, meshes facilitate profound geometric data fusion by utilizing both LiDAR points and Multi-View Stereo points for the geometric reconstruction.

Nowadays, joint photogrammetric and LiDAR acquisition is state of the art for airborne systems (hybrid acquisition). Recently, the joint orientation of LiDAR data and aerial imagery became feasible (hybrid adjustment). Concerning the recent hybridization trend, from our point of view, enhancing 3D point clouds to textured meshes may replace unstructured point clouds as default representation for urban scenes in the future. Notwithstanding, textured meshes are a mostly overlooked topic in the domain of photogrammetry and remote sensing despite their advantageous characteristics. For these reasons, we investigate the semantic segmentation of textured meshes in urban areas as generated from LiDAR data and oblique imagery. Moreover, we propose a holistic geometry-driven association of entities across modalities aiming at joint multi-modal semantic scene analysis (see Figure 10). Due to its integrative character, we choose the mesh as the core representation that also helps to solve the visibility problem for points in imagery.

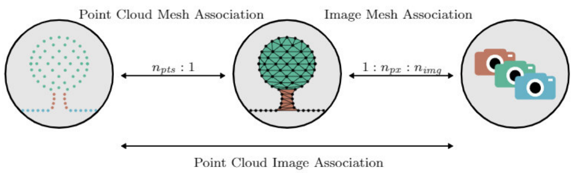

(a) Point Cloud Mesh Association (PCMA)			
	Mesh $\mapsto$ PC ($1 : n_{pts}$)	PC $\mapsto$ Mesh ($n_{pts} : 1$)	
Feature Transfer	Copy Value	Median Aggregation	
Label Transfer	Copy Value	Majority Vote	
(b) Image Mesh Association (ImgMA)			
	Mesh $\mapsto$ Img ($1 : n_{px} : n_{img}$)	Img $\mapsto$ Mesh ($n_{img} : n_{px} : 1$)	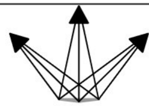
Feature Transfer	Copy Value	Median Aggregation	
Label Transfer	Copy Value	Majority Vote	
(c) Point Cloud Image Association (PCImgA)			
	PC $\mapsto$ Img	Img $\mapsto$ PC	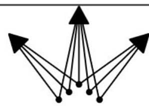
Feature Transfer	Median Aggregation	Median Aggregation	
Label Transfer	Majority Vote	Majority Vote	

Figure 10: Overview of the entire method that enables "juggling with representations": For each association mechanism, the transfer operations are given in dependence of information type (feature or label) and the transfer direction. The transfer directions use the following abbreviations: Point Cloud (PC) and imagery (Img). The pictograms on the right depict the linking of the respective entities. PCImgA provides two association modes: implicit and explicit linking. (a), (b), and the implicit version of (c) are face-centered. The relationship of implicit PCImgA is described by n_{pts}: 1: n_{px}: n_{img}. The explicit version is pixel-centered ($PC \mapsto Img$: n_{pts}: 1: n_{img}) or point-centered ($Img \mapsto PC$: n_{img}: n_{px}: 1).

Utilizing the proposed multi-modal fusion as the backbone and considering the established entity relationships, we enable the sharing of information across the modalities imagery, point cloud, and mesh in a two-fold manner: (i) feature transfer and (ii) label transfer. Consequently, we facilitate the training of machine learning algorithms and the (consistent) semantic segmentation of these modalities while reducing the manual labeling effort – both in a multi-modal and single-modal sense.

Figure 11 demonstrates the effectiveness of our methodology by example of label transfer on two data sets with significantly different scales and resolutions. Deploying our association algorithm, we can easily transfer information (in this case: labels) from a manually annotated point cloud to the mesh, and therefrom, to imagery (and vice versa). More importantly, by utilizing our mechanism, we enhance per-entity feature vectors with available features of other representations (multi-modality). The transferred labels and multi-modal feature vectors are input data for machine learning classifiers to achieve the semantic segmentation task.

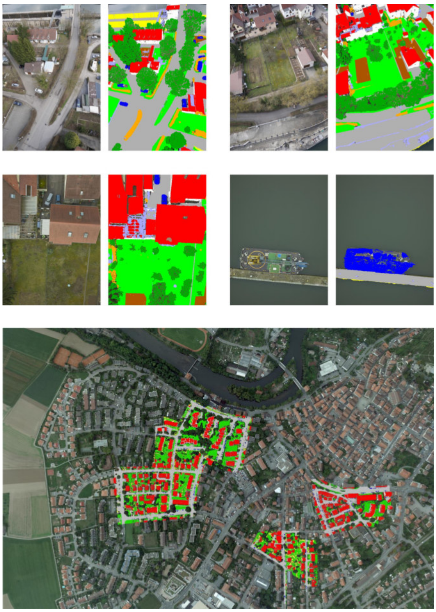

Figure 11: Automatically annotated imagery with labels as transferred from the manually annotated point cloud to the mesh and, therefrom, to image space (implicit PCImgA) for oblique (top) and nadir (center, bottom) images (GSD $\in$ of {2 cm, 3 mm, 8 cm}). Non-associated pixels are depicted with RGB values. Original RGB images are shown on the left except for the nadir image at the bottom, which covers the entire labeled area. The method cannot solve issues due to time shifts during acquisition (see cars at the center left example).

Towards Urban Tree Recognition in Airborne Point Clouds with Deep 3D Single-Shot Detectors

Automatic mapping of individual urban trees is increasingly important to city administration and planning. Although deep learning algorithms are now a standard methodology in computer vision, their adaption to individual tree detection in urban areas has hardly been investigated so far. We use a deep single-shot object detection network to find urban trees in point clouds from airborne laser scanning (Figure 12). The network consists of a sparse 3D convolutional backbone for feature extraction and a subsequent single-shot region proposal network for the actual detection. It takes as input raw 3D voxel clouds, discretized from the point cloud in preprocessing. Outputs are cylindrical tree objects paired with their detection scores. We train and evaluate the network on the ISPRS Vaihingen 3D Benchmark dataset with custom tree object labels.

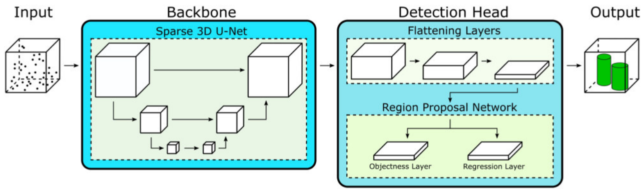

Figure 12: Network architecture.

The network achieves promising results compared to a traditional 2D baseline using watershed segmentation. It outperforms the baseline in terms of true positives, false negatives and positional RMSE, but needs improvement regarding height accuracy. All trees are accurately found in the augmented training set, based on the very good average precision (AP) for lower intersection-over-union (IoU) decision thresholds (Figure 13). However, the regressed parameters apparently do not fit as well, as shown by the decline in AP for higher IoU. The network does not perform as well on the test set, which indicates that the training set is not sufficiently large enough for a task like this, although it this overfitting was much less for semantic segmentation on the same dataset.

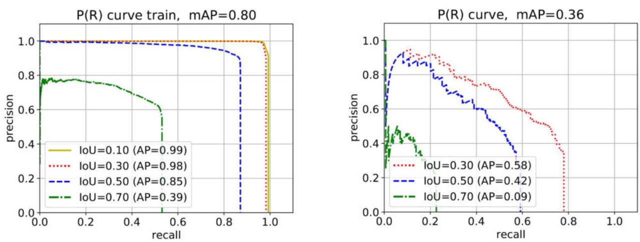

Figure 13: P(R) curves for the augmented training and the test dataset.

H3D - Hessigheim 3D: Benchmark on Semantic Segmentation of High-Resolution 3D Point Clouds and Meshes from Airborne LiDAR and Multi-View-Stereo-Image-Matching

In cooperation with other researchers, the Institute for Photogrammetry applied successfully for a ISPRS scientific initiative by proposing the benchmark Hessigheim 3D. This benchmark aims on the semantic segmentation of high-resolution 3D point clouds and meshes from airborne LiDAR and Multi-View-Stereo-Image-Matching.

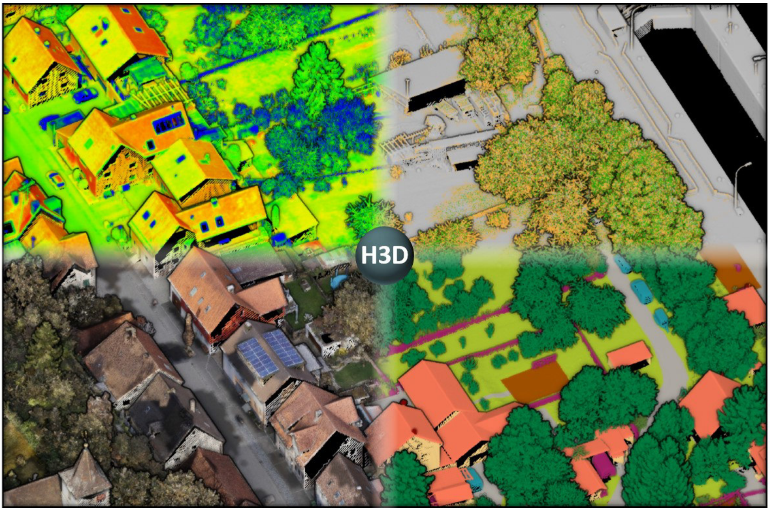

Further information on data, scope and how to participate can be found at the benchmark website https://ifpwww.ifp.uni-stuttgart.de/benchmark/hessigheim/default.aspx

References 2020

Bolz, T., Schmitz, S., Thiele A., Sörgel, U., Hinz, S.: Analysis of Airborne SAR and InSAR Data for Coastal Monitoring. 40. Wissenschaftlich-Technische Jahrestagung der DGPF in Stuttgart - Publikationen der DGPF, Band 29, 457-461.

Brockmann, H., Sörgel, U., Havel, P., Röpel, L., Cramer, M., Schneider, P.: Multisensorales ingenieurgeodätisches Bauwerks- und -umfeldmonitoring. Dresdner Wasserbauliche Mitteilungen.

Budde, L. E., Schmohl, S., Sörgel, U.: Unsicherheitsauswertung von semantischer Segmentierungen mittels Neuronaler Netze. 40. Wissenschaftlich-Technische Jahrestagung der DGPF in Stuttgart - Publikationen der DGPF, Band 29, 280-289.

Cramer, M., Havel, P.: UAV und Monitoring: Widerspruch oder erweiterte Option? UAV 2020 - The Sky is the Limit? DVW-Schriftenreihe, Band 97, Augsburg, S. 163-176.

Cramer, M., Kölle, M., Haala, N., Havel, P.: Flächenhaftes UAV-Monitoring: das Hessigheim-Projekt. Allgemeine Vermessungsnachrichten (avn) 03/2020, 107-117.

Cramer, M., Zhang, S., Meißner, H., Reulke, R.: Quality assessment of high-resolution UAV imagery and products. 40. Wissenschaftlich-Technische Jahrestagung der DGPF in Stuttgart - Publikationen der DGPF, Band 29, 33-46.

Doneus, M., Mandlburger, G., Doneus, N.: Archaeological Ground Point Filtering of Airborne Laser Scan Derived Point-Clouds in a difficult Mediterranean Environment. Journal of Computer Applications in Archaeology, 3(1), 92-108.

Haala, N., Kölle, M., Laupheimer, D.: Integrating UAV-based LiDAR and Photogrammetry. GIM International May 2020, 34(3), 10-13.

Haala, N., Kölle, M., Cramer, M., Laupheimer, D., Mandlburger, G., Glira, P.: Hybrid Georeferencing, Enhancement and Classification of Ultra-High Resolution UAV LiDAR and Image Point Clouds for Monitorig Applications. ISPRS Ann. Photogramm. Remote Sens. Spatial Inf. Sci., V-2-2020, 727-734.

Hadas, E., Kölle, M., Karpina, M., Borkowski, A.: Identification of Peach Tree Trunks from Laser Scanning Data Obtained with Small Unmanned Aerial System. ISPRS Ann. Photogramm. Remote Sens. Spatial Inf. Sci., V-2-2020, 735-740.

Kölle, M., Walter, V., Schmohl, S., Sörgel, U.: Hybrid Acquisition of High Quality Training Data for Segmentation of 3D Point Clouds Using Crowd-based Active Learning. ISPRS Ann. Photogramm. Remote Sens. Spatial Inf. Sci., V-2-2020, 501-508.

Kölle, M., Walter, V., Schmohl, S., Sörgel, U.: Evaluierung der Leistungsfähigkeit der Crowd f ür das Labeln von 3D-Punktwolken im Kontext von Active Learning. 40. Wissenschaftlich-Technische Jahrestagung der DGPF in Stuttgart - Publikationen der DGPF, Band 29, 299-311.

Laupheimer, D., Shams Eddin, M. H., Haala, N.: On the Association of LiDAR Point Clouds and Textured Meshes for Multi-Modal Semantic Segmentation. ISPRS Ann. Photogramm. Remote Sens. Spatial Inf. Sci., V-2-2020, 509-516.

Laupheimer, D., Shams, M. H., Haala, N.: The Importance of Radiometric Feature Quality for Semantic Mesh Segmentation. 40. Wissenschaftlich-Technische Jahrestagung der DGPF in Stuttgart - Publikationen der DGPF, Band 29, 205-218.

Mandlburger, G.: Möglichkeiten und Grenzen der Bathymetrieableitung mittels Single Photon LiDAR. 40. Wissenschaftlich-Technische Jahrestagung der DGPF in Stuttgart - Publikationen der DGPF, Band 29, 335-345.

Mandlburger, G., Pfennigbauer, M., Schwarz, R.: Genauigkeits- und Performanceuntersuchung eines neuen bathymetrischen UAV-Laserscanners. 40. Wissenschaftlich-Technische Jahrestagung der DGPF in Stuttgart - Publikationen der DGPF, Band 29, 321-334.

Mandlburger, G., Pfennigbauer, M., Schwarz, R., Flöry, S., Nussbaumer, L.: Concept and Performance Evaluation of a Novel UAV-Borne Topo-Bathymetric LiDAR Sensor. Remote Sens. 2020, 12(6), 28p.

Meißner, H., Cramer, M., Reulke, R.: Evaluation of Structures and Methods for Resolution Determination of Remote Sensing Sensors. In: Dabrowski J., Rahman A., Paul M. (eds) Image and Video Technology. PSIVT 2019. Lecture Notes in Computer Science, 11994, 59-69.

Nübel, H., Mandlburger, G., Kölle, M., Sörgel, U.: Bathymetrieableitung aus multispektralen Luftbildern über Convolutional Neural Networks. 40. Wissenschaftlich-Technische Jahrestagung der DGPF in Stuttgart - Publikationen der DGPF, Band 29, 156-171.

Rothermel, M., Gong, K., Fritsch, D., Schindler, K., Haala, N.: Photometric Multi-View Mesh Refinement for High-Resolution Satellite Images. ISPRS Journal of Photogrammetry and Remote Sensing, 166, 52-62.

Schmohl, S., Tutzauer, P., Haala, N.: Stuttgart City Walk: A Case Study on Visualizing Textured DSM Meshes for the General Public Using Virtual Reality. PFG - Journal of Photogrammetry, Remote Sensing and Geoinformation Science, 88(1), 1-8.

Schneider, P., Sörgel, U.: Monitoring einer Schleuse mittels satellitengestützter DInSAR-Techniken. 40. Wissenschaftlich-Technische Jahrestagung der DGPF in Stuttgart - Publikationen der DGPF, Band 29, 448-456.

Schneider, P. J., Sörgel, U.: Monitoring einer Schleuse mittels Persistent-Scatterer-Interferometrie. avn - allgemeine vermessungsnachrichten, 3, 118-123.

Schneider, P. J., Khamis, R., Sörgel, U.: Extracting and Evaluating Clusters in DInSAR Deformation Data on Single Buildings. ISPRS Ann. Photogramm. Remote Sens. Spatial Inf. Sci., V-3-2020, 158-163.

Schwarz, R., Pfeifer, N., Pfennigbauer M., Mandlburger, G.: Depth Measurement Bias in Pulsed Airborne Laser Hydrography Induced by Chromatic Dispersion. In: IEEE Geoscience and Remote Sensing Letters, doi: 10.1109/LGRS.2020.3003088.

Walter, V., Kölle, M., Yin, Y.: Evaluation and Optimisation of Crowd-based Collection of Trees from 3D Point Clouds. ISPRS Ann. Photogramm. Remote Sens. Spatial Inf. Sci., V-4-2020, 49-56.

Yin, Y., Walter, V., Kölle, M.,: Entwicklung und Evaluierung eines Web-Tools zur bezahlten crowd-basierten Erfassung von Bäumen aus 3D-Punktwolken. 40. Wissenschaftlich-Technische Jahrestagung der DGPF in Stuttgart - Publikationen der DGPF, Band 29, 478-487.

Zhang, S., Liu, C., Haala, N.: Three-Dimensional Path Planning of UAVs Imaging for Complete Photogrammetric Reconstruction. ISPRS Ann. Photogramm. Remote Sens. Spatial Inf. Sci., V-1-2020, 325-331.

Doctoral Theses

Cavegn, S.: Integrated Georeferencing for Precise Depth Map Generation Exploiting Multi-Camera Image Sequences from Mobile Mapping. Deutsche Geodätische Kommission, Reihe C, Nr. 863, München 2020.

Tutzauer, P.: On the reconstruction, interpretation and enhancement of virtual city models. Deutsche Geodätische Kommission, Reihe C, Nr. 851, München 2020.

Master Theses

Basile, D.: Crowdbasierte Erfassung von Fahrzeugen mithilfe eines mehrskaligen Ansatzes. Supervisors: Walter, V., Kölle, M.

Lansche, L.: 2D-Modellierung von Weinreben unter Verwendung verschiedener Machine Learning Methoden. Supervisors: Schmohl, S., Haala, N.

Nied, F.: Bildsegmentierung auf Basis des optischen Flusses. Supervisors: Schwarzenberg, G. (Robert-Bosch-GmbH), Haala, N.

Qiu, Z.: Geometry based rail track detection and blocking scenario identification using deep learning. Supervisor: Cramer, M.

Shiller, I.: Crowdbasierte Erfassung und Modellierung von Fahrzeugen aus 3D-Punktwolken. Supervisors: Walter, V., Kölle, M.

Suo, S.: Semantic Segmentation with Remote Sensing Data and Reference Labels Based on Simulation Methods. Supervisors: Auer, S. (DLR), Sörgel, U.

Tietz, V.: Masked Based 6D Vision Stixel Tracking. Supervisors: Müller, D. (Robert Bosch GmbH), Haala, N.

Wang, Z.: Domain Adaption for 3D Point Cloud Segmentation using Active Learning Strategies. Supervisors: Walter, V., Kölle, M.

Yuan, Y.: Investigation on Tailing Dam Deformations using differential SAR Interferometry Techniques. Supervisors: Schneider, P., Sörgel, U.

Bachelor Theses

Mayr, C.: DSM Inpainting using a Convolutional Neural Network. Supervisors: Rothermel, M. (ESRI), Haala, N.

Miehling, R.: Qualitätsuntersuchung zur GNSS/inertial-basieren Aerotriangulation am Beispiel einer empirischen UAV-Befliegung. Supervisor: Cramer, M.

Nübel, H.: Bathymetry from multispectral aerial images via Convolutional Neural Networks. Supervisors: Mandlburger, M., Kölle, M.

Zeng, H.: Personentracking mittels multisensorieller Daten für mobile Serviceroboter. Supervisors: Graf, F. (Fraunhofer IPA), Sörgel, U.

Zhang, Y.: Crowd-basierte Erfassung von Fahrzeugen aus 3D-Punktwolken. Supervisors: Walter, V., Kölle, M.

Activities in National and International Organizations

Cramer, M.:

Co-Chair ISPRS WG I/9: Integrated Sensor Orientation, Calibration, Navigation and Mapping

Mitglied im DIN Normungsausschuss NA 005-03-02 AA "Photogrammetrie und Fernerkundung"

Englich, M.:

Webmaster ISPRS

Haala, N.:

Chair ISPRS WG II/2: Point Cloud Generation

Chair EuroSDR Commission II: Modelling and Processing

Vorsitz DGPF Arbeitskreis Sensorik und Plattformen

Sörgel, U.:

President German Society for Photogrammetry, Remote Sensing and Geoinformation (DGPF)

Chair ISPRS WG III/3: SAR-Based Surface Generation and Deformation Monitoring

Walter, V.:

National Correspondent of the ISPRS Commission IV

Education - Lectures/Exercises

Bachelor "Geodäsie und Geoinformatik"

Geoinformatics I (Walter)	2/2
Geoinformatics II (Walter)	1/1
Image Processing (Haala)	2/1
Integrated Fieldworks (Haala, Hobiger, Sneeuw)	0/4
Introduction into Geodesy and Geoinformatics (Cramer, Hobiger, Sneeuw, Sörgel)	4/2
Photogrammetry (Cramer)	2/1
Remote Sensing (Sörgel)	2/1
Signal Processing (Sörgel)	2/1
Urban Planning (Dvorak)	2/0

Master Course "Geodäsie und Geoinformatik"

Aerotriangulation (Cramer)	1/1
Computational Geometry (Walter)	1/1
Computer Vision for Image-based Acquisition of Geodata (Haala)	1/1
Databases and Geographical Information Systems (Walter)	1/1
Digital Terrain Models (Haala)	1/1
Fundamentals in Urban Planning (Dvorak)	2/0
Georeferencing of photogrammetric Systems (Cramer)	1/1
Modelling and Visualisation (Haala)	1/1
Pattern Recognition and Image Understanding (Haala)	1/1
Remote Sensing (Sörgel)	1/1
Web-based GIS (Walter)	1/1

Master Course GEOENGINE

Airborne Data Acquisition (Cramer)	2/1
Computer Vision (Haala)	2/1
Geoinformatics (Walter)	2/2
Signal Processing (Sörgel)	2/1
Integrated Fieldworks (Haala, Hobiger, Sneeuw)	0/4
Pattern Recognition (Sörgel)	2/1
Remote Sensing (Sörgel)	2/1

Master Course "Infrastructure Planning"

Introduction to GIS (Walter)	2/0

Master Course "Aerospace Engineering"

Image Processing (Haala)	2/1
Introduction into projective Geometry (Cramer)	2/0